DESIGN AND EVALUATION OF A CONTINUUM ROBOT WITH EXTENDABLE BALLOONS

by

Efe Yamaç Yarbaşı

B.Sc., in Mechanical Engineering, Middle East Technical University, 2012

Submitted to the Institute for Graduate Studies in
Science and Engineering in partial fulfillment of
the requirements for the degree of
Master of Science

Graduate Program in Mechanical Engineering

Boğaziçi University

2016

ACKNOWLEDGEMENTS

I would like to thank my advisor, Professor Samur for his wisdom, support and patient guidance which enabled me to complete this work. He has always been a source of inspiration to me as a researcher during my time at Boğaziçi University.

I would also like to thank Prof. Başẗurk and Prof. Akar for accepting to be members of jury committee despite their tight schedules. I am also thankful to Prof. Yılmaz for his constructive criticism and priceless advise.

I am grateful to my colleagues at Haptics and Robotics Laboratory, my friends Onur Yüksel, Onur Deniz Uysal and my cousins Deniz Özdamar and Helin Uluca. I would like to express a special thanks to my girlfriend Gökçin Çınar who encouraged, supported and made me happy from all the way the other side of the world during my studies.

Finally, I wish to thank my mother Nevra, my father Adnan, my grandmother Muzaffer and my sister Irmak for their everlasting love and support.

ABSTRACT

DESIGN AND EVALUATION OF A CONTINUUM ROBOT WITH EXTENDABLE BALLOONS

In this thesis, a novel continuum robot actuated with extendable balloons is presented. The robot is composed of two parts; the tip and the flexible shaft. The balloons are attached to the tip from their slack sections. The utilized balloons are able to extend much in length without having a significant change in diameter. Employing two balloons in an axially extendable, radially rigid flexible shaft, radial strain becomes constricted; allowing free elongation. As inflated, the balloons apply a force on the wall of the tip, on which they are attached. This force pushes the tip forward, enabling the robot to elongate in longitudinal direction and take some of the slack back. The air is supplied to the balloons by an air compressor and its flow rate to each balloon can be independently controlled by solenoid valves via Pulse Width Modulation (PWM) signals. Changing the air volumes differently in each balloon orients the robot, allowing navigation in substantially long and narrow environments. Mechanical properties of different balloons are analyzed during inflation. Afterwards, the robot is subjected to open field and maze-like environment navigation tests. The proposed type of robots can be used in many applications such as exploratory or medical purposes by having necessary tools attached to the tip.

ÖZET

UZAYABİLEN BALONLU BİR SÜREM ROBOTUN TASARIMI VE DEĞERLENDİRİLMESİ

Bu tezde, uzayabilen balonlar tarafından çalıştırılan özgün bir sürem robotu sunulmuştur. Robot iki kısımdan oluşmaktadır; uç ve esnek şaft. Balonlar gevşek kısımlarından uca iliştirilmiştir. Kullanılan balonlar, çaplarında kayda değer bir değişme olmadan büyük miktarlarda uzayabilmektedir. İki balon boylamasına uzayabilen ama radyal olarak esnemeyen, uzayabilen bir şaftın içine yerleştirildiğinde, radyal uzama kısıtlanmakta ve serbest uzama sağlamaktadır. Balonlar şiştikçe bağlı oldukları uç kısma bir kuvvet uygulamaktadırlar. Bu kuvvet ucu ileri doğru iter ve robotun boylamasına uzamasını ve gevşek kısmın bir miktarını geri çekmesini sağlar. Balonlara hava, bir hava kompresörü ile verilmekte ve bu havanın akış miktarı her balon için bağımsız olarak solenoid vanalara verilen Darbe Genişlik Modülasyonu sinyalleri ile kontrol edilmektedir. Balonlardaki hava hacmini farklı miktarlarda değiştirmek robotun dönmesini ve dolayısıyla özellikle uzun ve dar ortamlarda yönlendirilmesine olanak sağlamaktadır. Şişme sırasında balonların mekanik özellikleri analiz edilmiştir. Önerilen robot tipi, keşif veya tıbbi amaçlar gibi birçok uygulamada kullanılabilir.

TABLE OF CONTENTS

LIST OF FIGURES

LIST OF TABLES

LIST OF SYMBOLS

A	Cross-sectional Area
L	Length of the cylinder
n	Moles of air in the cylinder
P	Pressure
R	Ideal Gas Constant
V	Volume of the cylinder
T	Temperature

LIST OF ACRONYMS/ABBREVIATIONS

2D	Two Dimensional
3D	Three Dimensional
DOF	Degree of Freedom
ER	Electro Rheological
HRI	Human Robot Interaction
MR	Magneto Rheological
PAM	Pneumatic Artificial Muscles
pHRI	Physical Human Robot Interaction
PWM	Pulse Width Modulation
SEA	Series Elastic Actuator
SMA	Shape Memory Alloy

1. INTRODUCTION

1.1. Motivation

In order to achieve a high level of precision, rigidity of robots has long been used as an optimization criterion [1]. This resulted in very stiff robots that consist of rigid links. These robots are successful for most application fields such as manufacturing automation where humans and robots do not come into contact in a working environment [2] . However, there are cases where rigid robots are simply ineffective or even dangerous to work with. In order to tackle these problems, flexible robots are being developed. Flexible robots consist of flexible links or joints. They are able to address interactive manipulation tasks with a certain level of intrinsic security [1]. In fields like endoscopic surgery for instance, where the purpose is to navigate the endoscope tip in a three-dimensional body cavity by using manual steering requires physical contact between the patient and the robot. Traversing tortuous trajectories with a rigid tool may damage the surrounding tissues or even be impossible. A flexible structure would allow robots to navigate inside the body and perform tasks without damaging delicate surroundings. However, structural flexibility also introduces instability, making it harder to control the robot [3]. Specific maneuver techniques that require experience and expertise should be applied. Moving the tip to a specific location requires a combined insert, roll and articulation input that is complex and somewhat arbitrary [4]. Considering the complications and disadvantages of manual steering, developing a flexible robotic system that can be easily guided for this kind of medical applications can have a dramatic effect on reducing complications such as tissue perforation, discomfort, hemorrhage and the time cost of the operations [5]. The idea of designing and developing a robot that can be easily guided through delicate and unstructured environments such as exploratory or medical applications was the motivation that led to this study.

1.2. Approach

Current state of the art robots, even though they may be flexible, have some problems such as lack of compliance [6], insufficient dexterity, not being able to work in unstructured environments [7] etc. The goal of this study is to develop a novel soft continuum robot which can be utilized in various applications where the objective is to reach a goal position and carry out tasks there, without applying much force to the walls of the cavities. In order to fulfill these requirements, aims listed below were followed:

Aim 1: Design a soft continuum robot with extendable balloons.

Aim 2: Analyze the mechanical characteristics of the balloons that are to be used for actuation.

Aim 3: Develop a pneumatic system utilizing air pumps and solenoid valves to control the air volume in the balloons.

Aim 4: Measure the forces that can be applied by the robot and navigate the robot in a desired way.

1.3. Outline

In this thesis, the process of design and evaluation of this robot is presented. First, related studies in the literature are reviewed and analyzed in detail. Then, conceptual design is discussed. Afterwards, the critical components used in the system and the whole experimental setup are explained. Experimental results are presented and discussed. Finally, a detailed conclusion is made, future work and potential applications are discussed.

2. LITERATURE REVIEW

Since the dark ages, mankind have been making use of tools to manipulate objects in ways that their bodies do not allow. Over millennia, these tools have been continuously modified and developed to adapt to the changing tasks and complete them more successfully. In the last century, some of the tools that have been developed has taken the shape of robots. Even though emerging of the idea of the first so-called robot can be dated back to Ancient Greece [8], only in the last century did the robots start to have a significant effect on the world. How we utilize robots, has a great and exponentially increasing impact on modern life.

Robotics is defined as the "science of designing and operating robots" [9]. The main purpose of robotics is to design and manufacture robots that can complete challenging tasks that require more speed, strength or precision than a human can provide or to assist a human complete such a task. Since performance of robots is improving drastically, they are taking place in various fields like military [10], mining [11], manufacturing [12] and medicine [13] .

In order to achieve the aims noted in Section 1.2, related studies have been reviewed. This chapter covers the important parts of these studies that have been beneficial in different steps of this research.

2.1. Background for Flexible Robotics

As stated in Section 1.1, there are limitations of utilizing rigid-body robots in many cases. Thus, researchers has been working on adding some amount of flexibility to robots to perform better in certain tasks [1] especially in fields like physical Human Robot Interaction (pHRI), where humans and robots are in physical contact.

The simplest way of introducing flexibility to a robot is to pad it with some kind of soft material [2] so that compliance of the system is increased. The RI-MAN [14]

can be considered a good example for this case. RI-MAN is a human-interactive robot built for carrying humans and it consists of rigid links and joints. The arms are padded so that there is some compliance on the arm, increasing the comfort while carrying a person.

Another way of introducing flexibility is to utilize flexible joints. This is the most common type of flexibility encountered in robots, due to transmission elements such as harmonic drives, cables, gears [2] etc. For example, the Series Elastic Actuators (SEA) [15] introduces compliance between link and actuators to reduce impedance of stiff actuators. Further research has been conducted to provide inertial decoupling between actuator and link during impacts by making use of joint flexibility [16].

Another component of a robot that can be utilized to introduce flexibility is their links. Flexible link robots and manipulators have been around for some time. However, introducing flexible links introduce control problems as well. Many researchers propose various control methods for flexible link methods for couple of decades and it is still among the popular topics to conduct a research on [17–19].

A relatively newer branch of robotics is $Soft\ Robotics$. This branch deals with soft robots, generally very compliant and lightweight systems. It is expected that this type of robots will start working in the vicinity of and together with humans, an opinion shared by many researchers and industry professionals. In order to reach the expected performance and safety during interaction with humans or in unknown environments, rich sensory information, lightweight design and soft-robotic features will be required [20]. In these robots, lack of stiffness adjustment and controllability issues are the biggest challenges [21]. Therefore, there has been lots of research going on to tune stiffness of robots making use of methods such as using granular jamming [22–24], $electro-rheological$ (ER) fluids [25], $magneto-rheological$ (MR) fluids [26]. Another perspective in this field is that of the materials point of view. Researchers have been studying the characteristics of the deformable materials that are used in soft robots and categorizing them [27]. A very popular robot in the field is the STIFF-FLOP, a soft manipulator with variable stiffness [24]. STIFF-FLOP has a modular structure,

which has elastomer chambers located about the axial axis and can be navigated to a desired position by controlling the air volumes in these chambers.

Continuum robots are a new class of soft, continuous backbone robot manipulators [28]. They are moved via deformation of this backbone. This class utilizes hyperelastic structures like special polymers that tolerate high strains. Theoretically, they have infinite degrees of freedom. Even in reality, they have a high number of potential actuatable degrees of freedom [29]. They utilize compliance to achieve motion, offering distinct advantages [2]. In his paper, Walker discusses the common problems of continuum robots [21]. Inherently complex kinematics because of the continuous structure, structural stiffness issues and underactuated designs makes it challenging to design and control a continuum robot.

2.2. Biological Inspiration for Continuum Robots

Many of the robots developed mimic the movements of either humans or other animals in the nature. Most of the continuum robots are inspired from examples in the nature, especially muscular-hydrostats. Muscular-hydrostats are organs which lack typical systems of skeletal support [30]. Some organs of animals, including the mammal and lizard tongues, elephant trunks and appendages of cephalopods can be considered in this class. In their paper, Kier and Smith(1985) discuss the biomechanics of movements of these organs in detail. In this section, the biomechanical properties of such organs are discussed, according to this paper.

Muscular-hydrostats are organs that are composed of almost entirely of muscles. Normally, the skeletal system transmits the force generated by contracting muscles and allow them to return to their resting lengths. It also provides support to compressive and bending forces and amplify the resultant force, speed or displacement of muscular activity. However, muscular-hydrostats are independent of the skeletal system. It is interesting to see that these organs are capable of successfully completing challenging tasks very effectively without the support of skeletal system.

A muscular-hydrostat has a group of closely packed 3D musculature. These muscle fibers are generally located perpendicular to the long axis, parallel to the long axis and helical or oblique around the long axis of the organ. Even though there are also nerves, blood vessels etc. in these organs, the main feature for movement is the muscles. The most important biomechanical feature of a muscular-hydrostat is that they have constant volume, no evidence has been found of a major fluid flow to these organs. With constant volume, these organs can perform elongation, shortening, bending, stiffening and torsion. For example, with the activity of muscles that lie parallel to the longitudinal axis, the organ will elongate. For a tongue, for example, this elongation can be up to 106%. However, since the volume is constant, the cross-sectional area will decrease. The relation between the length and cross-sectional area for a constant volume cylinder is demonstrated in Figure 2. This is the case with muscular-hydrostats as well. Bending is produced by the contraction of one of the muscle parallel to the longitudinal axis and the resistance of the other. If this resistance is not present, the organ will shorten instead of bending. However, since the muscles are working antagonistically, the change in cross-sectional area will be very little. Similarly, stiffening, shortening and torsion can be obtained by contraction of relevant muscles.

These mechanics have been a source of inspiration for researchers working in the field of soft robotics. Even though the nature of these organs are almost completely understood and the developed robots are getting better day by day, there is still a long way to go until the efficiency and the compactness of such organs is enhanced.

2.3. The Need for Soft Robots

Robots can be classified as hard or soft on the bases of compliance of their underlying materials [7]. Soft robots are a relatively new type of robots, being studied for about only three decades.

Most robots that are used today are hard robots. They utilize rigid links and joints. These robots are typically used to perform repetitive tasks with great precision. They also have high stiffness so that vibration and the deformation of their

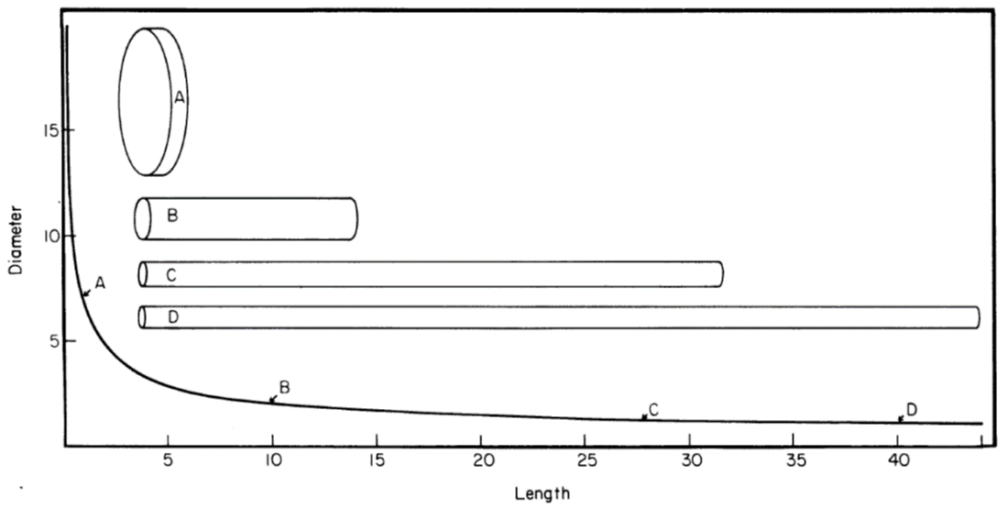

Figure 2.1. Plot of relation between length and diameter of a cylinder of constant volume. Reprinted from [30].

structure does not compromise accuracy of the task [7]. Each joint used typically introduce one more DOF to robot. With combination of all joint variables and link lengths, end-effector can be brought into the desired position and orientation. Some robots made of certain hard materials such as shape memory alloys (SMAs) can have continuous deformation and infinite DOF. This type of robots can be considered as hyper-redundant robots [29]. A hyper-redundant robot has a very large number of actuatable DOFs. These robots are also referred as "snake-like", "highly articulated" and "elephant trunk". Compared to typical hard robots, hyper-redundant robots have higher dexterity and they are able to work in unknown or *unstructured environments*-environments in where a robot cannot rely on a detailed and accurate model [31]. In Figure 2.2, a snake robot is shown navigating through an unstructured environment.

Soft robots also have hyper-redundancy, allowing the robot to take infinite number of shapes or configurations. Some of the advantages of soft robots are that they generate little resistance to compressive forces, allowing them to conform obstacles [7]

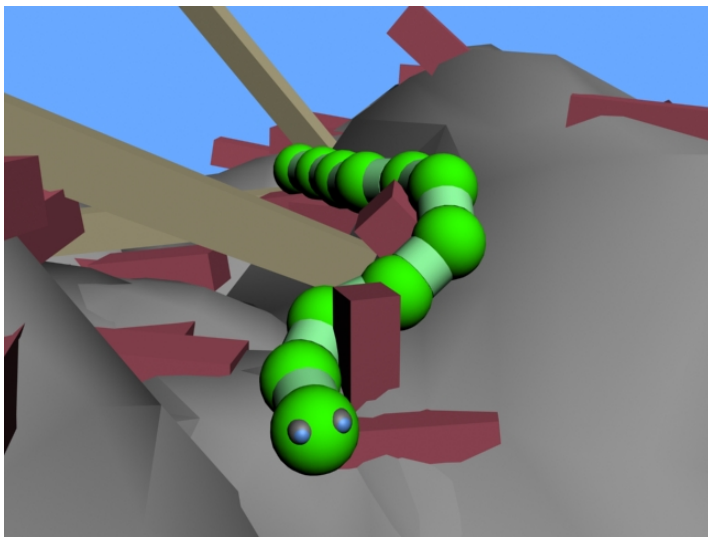

Figure 2.2. A snake robot navigating through an unstructured environment Reprinted from [32].

and they can use large strain deformation. Moreover, new soft matters have been synthesized and diverse fabrication techniques made these new soft matters commercially available [27]. In a hard robot, it is easy to sense the joint variables using encoders. The tip position and orientation can be found by using these joint variables and conducting a forward kinematics analysis. This is typically a very fast and accurate process. Inverse kinematics approach can also be used, if the configuration that would bring the end-effector to a desired position is to be found. All of the link positions can be calculated and they can be brought into necessary position. However, since it is not possible to have a motor to control every DOF like in hard robots, soft robots are underactuated. Some of the DOFs may be influenced by actuators but many of them not independently controllable. They bend continuously along their length via elastic deformation and produce motion through the generation of smooth curves [33]. This also brings the challenge of sensing and controlling the shape of the robot. How a continuum robot moves compared to rigid link robots is demonstrated in Figure 2.2.

To sum up, main advantages of soft robots over hard robots can be listed as:

- Infinite number of DOF due to hyper-redundancy, thus variety in available con-

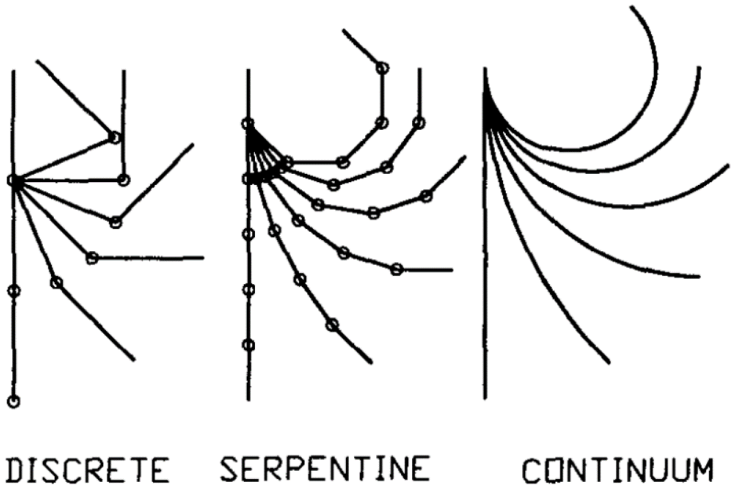

Figure 2.3. Different types of robot motion. Reprinted from [33].

Table 2.1. Characteristics of different types of hard (first three columns) and soft robots [7].

	Rigid	Discrete hyperredundant	Hard continuum	Soft
Properties				
df	Few	Large	Infinite	Infinite
Actuators	Few, discrete	Many, discrete	Continuous	Continuous
Material strain	None	None	Small	Large
Materials	Metals, plastics	Metals, plastics	Shape memory alloy	Rubber, electroactive polymer
Capabilities				
Accuracy	Very high	High	High	Low
Load capacity	High	Lower	Lower	Lowest
Safety	Dangerous	Dangerous	Dangerous	Safe
Dexterity	Low	High	High	High
Working environment	Structured only	Structured and unstructured	Structured and unstructured	Structured and unstructured
Manipulable objects	Fixed sized	Variable size	Variable size	Variablesize
Conformability to obstacles	None	Good	Fair	Highest
Design				
Controllability	Easy	Medium	Difficult	Difficult
Path planning	Easy	Harder	Difficult	Difficult
Position Sensing	Easy	Harder	Difficult	Difficult
Inspiration	Mammalian limbs	Snakes, fish		Muscular hydrostats

figurations

- High dexterity
- Little resistance to obstacles
- Safe Human Robot Interaction (HRI)
- Large strain deformations
- Ability to work in unstructured environments

2.4. Pneumatic Actuators and Inflatable Structures in Robots

Pneumatic actuators are devices that uses the potential energy of a compressed gas to generate mechanical motion. They offer advantages like low cost, high power-to-weight ratio, ease of maintenance, cleanliness, safe operation and ease of availability. They can be utilized in robotic applications such as position control of manipulators, end effectors and grippers. However, because of the nature of the gases, they are highly nonlinear and dead time due to compressibility of air can also be a problem when controlling [34]. They can be used in the field in manipulation tasks [35], telerobotics [36], haptic interfaces etc [37]. Pneumatic Artificial Muscles (PAMs) were developed as early as 50s under the name of *McKibben artificial muscles* [38]. These are mechanisms that contract or extend with the change in air pressure in their pneumatic bladder. They possess advantages like lightweight design, direct connection, easy replacement and safe operation. On the other hand, it is problematic to control the position accurately. However, much more effort has been put into PAMs recently so that it would be safe for one to assume that these control problems will be solved in near future [39].

Similar to PAMs, some inflatable structures are being used in robots as well. Generally, air is trapped in a membrane structure that can tolerate high strains. Since the pressure differential is high between internal end external pressures, high strains can be achieved. The deformation of this membrane can be used to position the structure [2]. Another advantage of these structures is the ability to be deployed so that their volume is less of a problem. There has been some robotic applications as well. Salomonski et. al. (1995) have developed an inflatable structure for a robotic arm based on elements made of thin inflatable shells [40]. They attached an inflatable

forearm to a commercially available PUMA robot. This design improves the payload-to-weight ratio and allows easy transportability. Another example is the inflatable linkages developed [41], which is stated as a less expensive solution to problems inherent for inspection. The inflatable robotic finger developed by Qi et al. is also a good example of the range of inflatable mechanisms, having the potential of being a very practical and low-cost gripper in a robotic hand [42]. Its grasping capabilities are shown in Figure 2.4.

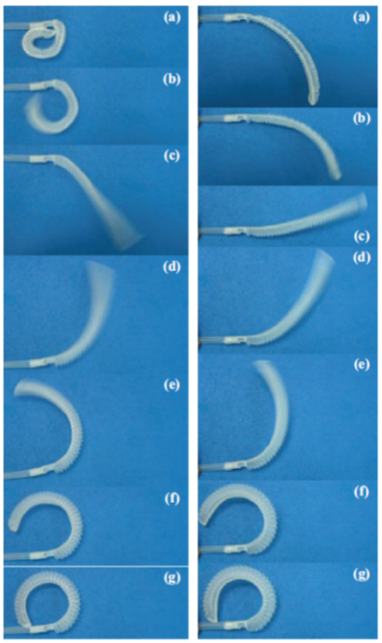

Figure 2.4. Elongation and bending of the inflatable finger developed by Qi et al. [43].

These studies prove that inflatable structures can successfully be utilized in robotics. Further research is going on to solve the control and sensing issues.

2.5. State of the Art in Continuum Robotics

As stated in Section 2.3, rigid-link robots have many shortcomings. After Chirikjian and Burdick have established the general backbone kinematics and dynamics for continuum robots [44] [45], the field attracted many researchers throughout the world. In this section, several state of the art continuum robots designed in last decades will be

discussed.

2.5.1. Tendon-Based Designs

The most direct approach to bending a continuous structure is the use of remotely actuated tendons [28]. A backbone will attain a given shape when it is not under any loading. Tendon-based continuum robots have tendons throughout the backbone, either in the middle or about the longitudinal axis. When a tendon is actuated from the base, resulting forces will make the robot to go into a bent state. This type of design is simple and straightforward to realize in hardware. In Figure 2.5, an elephant's trunk robot is demonstrated. It is bent to the side where the tendons are actuated.

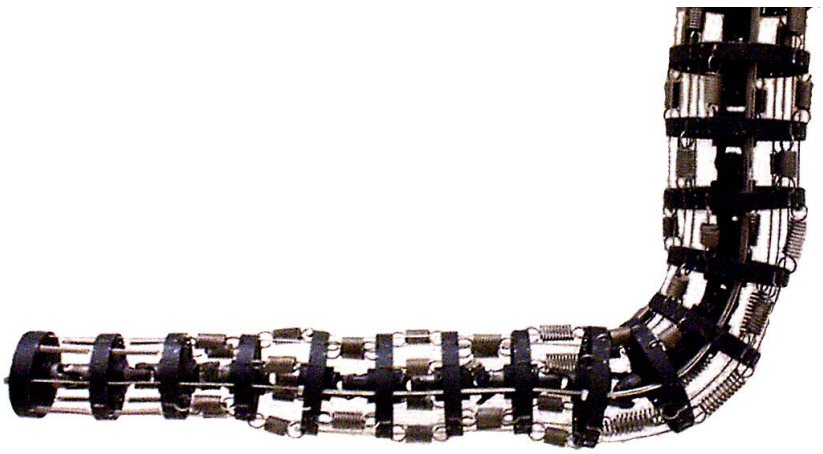

Figure 2.5. Elephant's trunk robot. Reprinted from [21].

In order to give the backbone some kind of compliance, compressible springs have been utilized in some robots. Tendril, a minimally invasive robot that is designed for in-space inspection [46] is a good example for this. However, this also results in some control problems as control effort intended for backbone bending is lost in compression [28]. A solution to this problem is to use an incompressible rod as the backbone but that will result in the loss of elongation and shortening abilities.

2.5.2. Concentric Tube Designs

Another approach to have actuation in continuum robots is to use concentric tubes in the backbone. This concept basically works as a telescope. By rotating the pre-curved tubes, desired orientation and position can be obtained. In Figure 2.6, the concept is demonstrated.

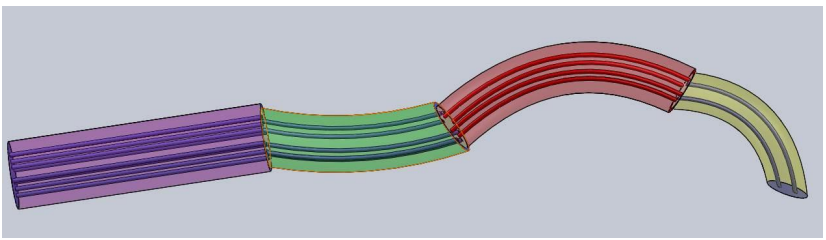

Figure 2.6. Concentric tube continuum robot concept. Reprinted from [28].

The bronchoscope developed by Swaney et al. utilizes both concentric tubes, tendon actuation and a bevel tip [47]. The device is thoroughly tested on a gelatin model and found successful. It is claimed that this device will be ready for clinical trials soon.

2.5.3. Locally Actuated Backbone Designs

In this type of design, the backbone is directly formed by the actuators. A locally actuated continuum robot is the closest to the biological continuum structures [28]. Typically, the backbone is formed by multiple sections, resulting in a modular structure. These modules are often independently actuated. McKibben muscles commonly seen in such examples [48].

A locally actuated continuum robot has a backbone that may be able to perform elongation, bending in 2D and torsion. This feature is not provided by tendons or concentric tubes [28]. However these designs have following disadvantages; complex structure, low force generation capabilities and the need for external pressure regulation equipment.

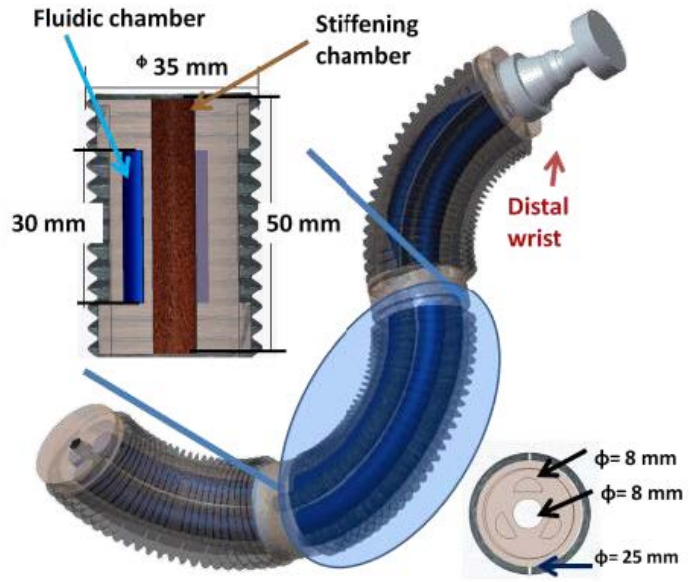

Figure 2.7. The STIFF-FLOP manipulator. Architecture of a module and cross-sectional view are also shown. Reprinted from [24].

The STIFF-FLOP manipulator (Figure 2.7) is a continuum robot that is being developed mainly for laparoscopic applications. This modular manipulator has three fluidic chambers about the longitudinal axis of the robot [49] [24]. The effect of pressurizing one chamber is demonstrated in Figure 2.8. In order to elongate the module, all three chambers are inflated. Inflating a chamber more than the others will result in bending of that module to the opposite direction. Further research is going on the module design of this robot to have improved actuation and sensing [50].

Most studies utilize fluidic chambers that are radially constricted by some kind of fiber. The design process is extensively studied by Bishop-Moser et al [51]. Currently, only hydraulic and pneumatic actuators combine bending and force generation capabilities for continuum robots at the human scale [28].

A bio-inspired manipulator is shown in Figure 2.9. This manipulator looks almost like an octopus arm and it is designed to work in a similar fashion. It has both tendon and pneumatic actuation [52]. It consists of three independently inflatable modules covered with some kind of fabric and twelve tendons are located around the fabric.

Figure 2.8. One of the air chambers of the STIFF-FLOP manipulator is inflated. Reprinted from [24].

When not rotated, it holds a conical shape. The ultimate goal for this robot is also laparoscopy.

2.5.4. Variable Stiffness In Continuum Robots

Continuum robots generally lack longitudinal compliance along the backbone independent of their actuation mechanisms. Even the pneumatically actuated ones suffer from this because pneumatic forces offer only a limited range of possible backbone stiffness [28]. In this section, several methods to overcome this problem are discussed in detail.

The first strategy to tackle the backbone stiffness problem is to making use of $electro-rheological$ (ER) fluids. These are smart fluids that transform into a solid-like state when an electric current is applied. By utilizing an ER fluid in the backbone, it is possible to vary the backbone stiffness and even lock the backbone in a desired position. In their study, Sadeghi et al. present the design of a ER valve that can be used to control the stiffness of soft robots and test it on a tendon driven continuum arm [25]. Another similar way is to use a $magneto-rheological$ (MR) fluid in the backbone. It is shown the a MR fluid actuator can be used to tune the stiffness of a 2 DOF rigid manipulator [26].

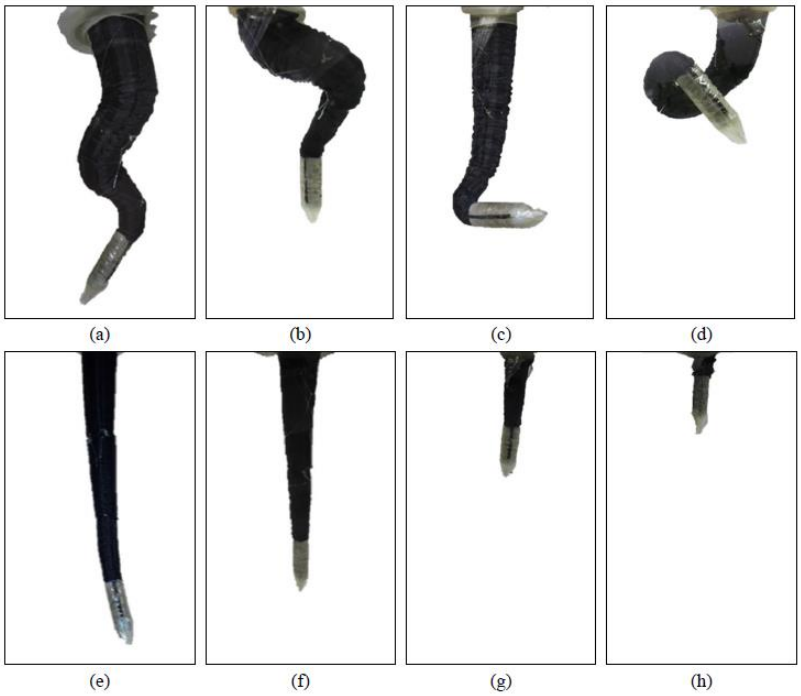

Figure 2.9. Different configurations of the octopus arm-like manipulator. Reprinted from [52].

Shape Memory Alloys (SMAs) are smart materials that are able to recover their original shape after severe elastic deformations when their temperatures are altered [53]. There are robots utilizing the continuous deformation characteristics of SMAs. For example, the Robojelly is a jellyfish robot that uses SMAs as actuators [54]. It has a bio-inspired design and mimics the muscular deformation of jellyfish by changing the curvature of tendons constructed of SMAs. Another example is the hyper-redundant planetary exploration robot developed by Sujan et al [55]. Each of its links is actuated by a pair of antagonistic SMA wires.

Another method used in variable stiffness continuum robot design is *jamming*. Jamming is obtained when a granular medium (such as sand or coffee grains) is packed in a close chamber and use vacuum to *jam* it into a solid-like state [28]. When the pressure is increased, the medium returns to a fluid-like state. The soft robotic spine developed by Wei et al, uses jamming method to control the stiffness of the robot [22].

They also examine the effects of grain size and state that different sized particles should be tested and optimized depending on the application. It can be said that using smaller grains could be better in terms of predictability since it fills more space but it brings a weight penalty that would have negative effect on load bearing capability as well. Another modular robot utilizing jamming, performing different tasks in jammed configurations is demonstrated in Figure 2.10.

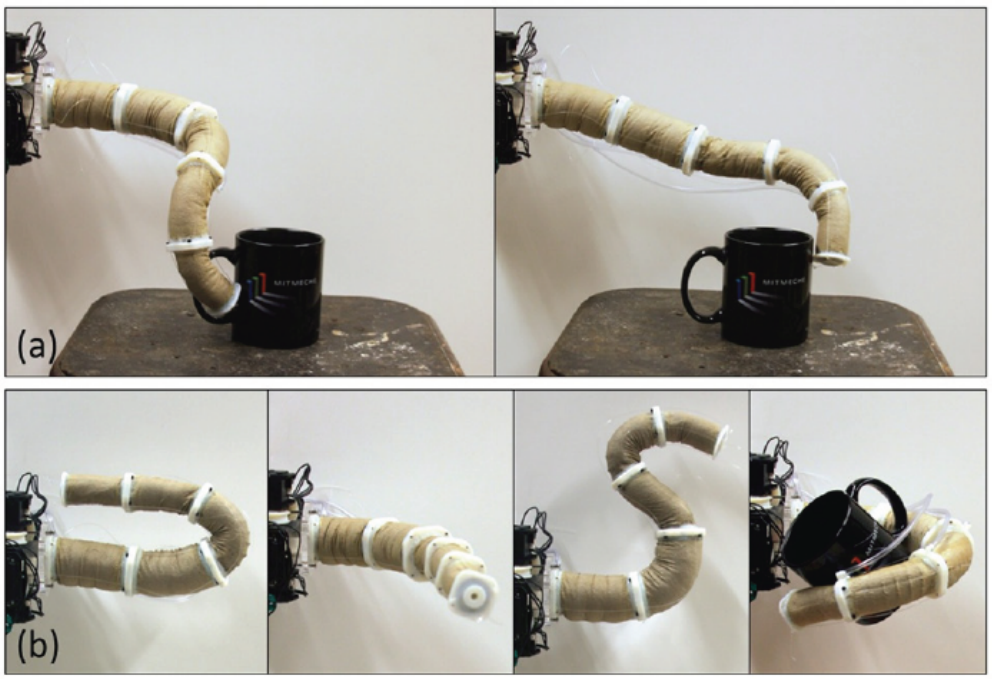

Figure 2.10. The manipulator demonstrating its ability to: (a) reach an end effector target with multiple configurations, and (b)achieve many complex and highly articulated shapes. Note that the manipulator is jammed to rigidly hold its shape in all these images. Reprinted from [23].

3. CONCEPTUAL DESIGN

As stated in Section 1.2, the motivation in this thesis is to design and develop a robot that can be easily guided through delicate and unstructured environments like in endoscopic operations. With insufficient amount of compliance or available configurations, excessive forces may occur especially around the regions that are in contact with the obstacles or the environment. However, this problem can be avoided if the robot is able to change it shape according to the environment it is being navigated in. For this purpose, the primary requirement was that the robot would conform the obstacles so that no excessive force is to be applied on the surroundings.

3.1. Initial Trials

Our initial idea was to use an unfolding industrial cable carrier-like mechanism. It was supposed to unfold itself on the surrounding periphery and create a stable platform from which it can continue unfolding further. However, it did not have any compliance in one transversal direction, making it hard to make any turns in that direction. Another problem was that, it required more than twice of the cross sectional area of the cable carrier to go through, resulting in a bulky design. Afterwards, another concept of using a chain wrapped single-speed gear was tested. The idea was to roll a single-speed gear forward by also rotating it. However, it was not possible since the chain is not a mechanical component that resists to compressive forces. The chain buckled and the gear did not go further as planned. When we were thinking of another design, we encountered a video that included extendable balloons. The idea of using extendable balloons looked very promising.

3.2. Extendable Balloon Concept

It is seen that these balloons are able to elongate when inflated as shown in Figure 3.4. Our thought was to attach a tip section to the distal end of the inflated section of the balloon and keeping the slack section on the other side of the tip as it can be

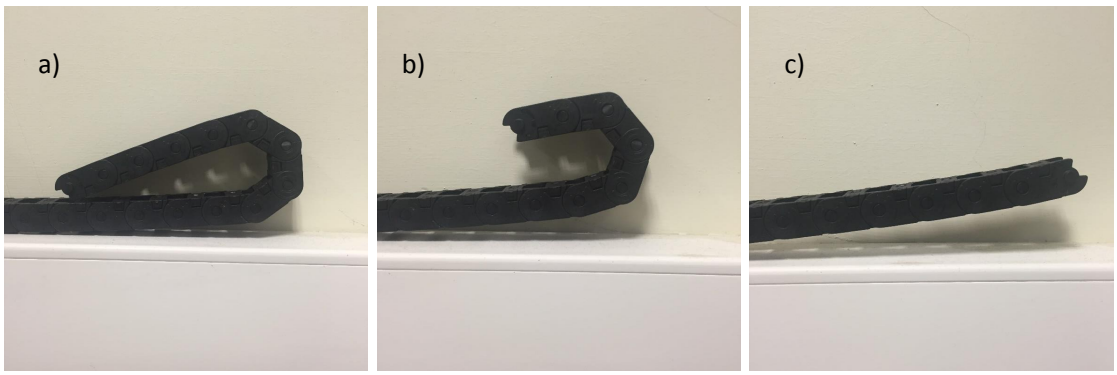

Figure 3.1. Cable carrier unfolding as it goes forward.

seen in Figure 3.3. As the balloon inflates, the force generated on the wall of the tip will push it forward allow some of the slack will slide backwards. If multiple balloons are used and if they are restricted in the radial directions, only longitudinal strain will take place.

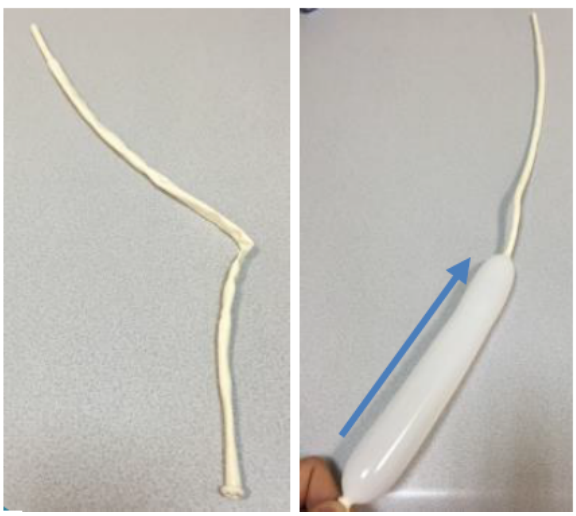

Figure 3.2. Inflation of an extendable balloon.

For this study, a 2D planar motion is satisfactory, therefore two balloons are used. Positioning their inlets in the same place, constricting them radially in a flexible extendable shaft and making sure that their distal inflated sections have contact with

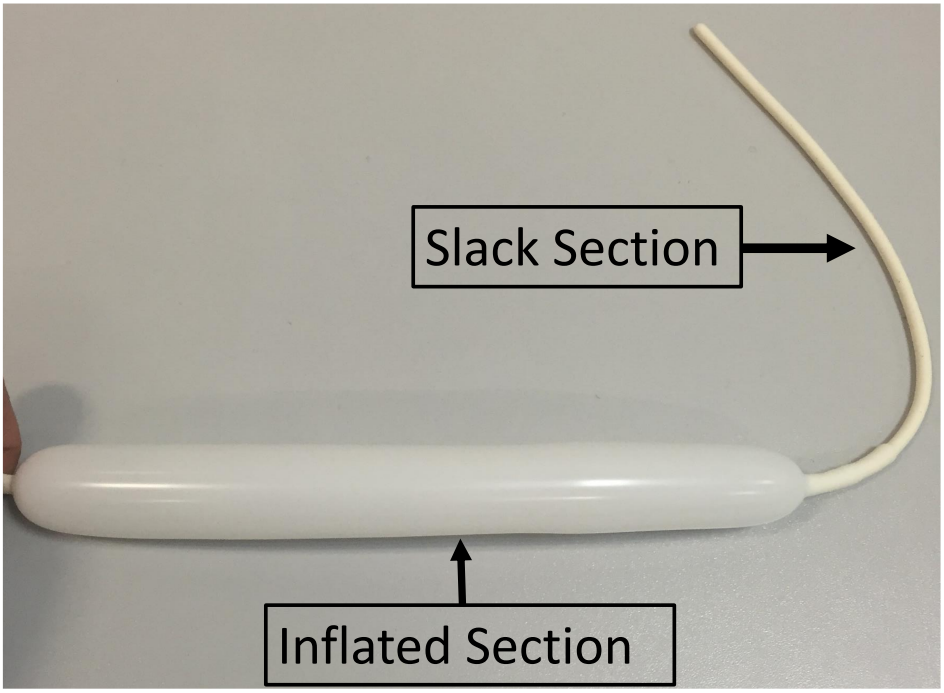

Figure 3.3. When an extendable balloon is inflating, slack section remains at the distal end.

the same part -tip- will result in a constricted continuum mechanism. Similar to the examples found in the nature discussed in section 2.1, this mechanism will be able to elongate and bend. However, elongation will not result in a decrease in diameter since this is not a constant volume system.

Basic two motions, elongation and bending, will be obtained by inflating two balloons independently. For the robot to elongate, both balloons will be inflated at the same time. Elongation is demonstrated in Figure 3.4. For it to bend, one balloon has to have more air volume than the other one. It should be inflated while the other one is kept at the same volume or maybe even deflated. This behaviour is demonstrated in Figure 3.5. Deflating a balloon will result in a smaller radius turn.

Since the the robot has no backbone, it can easily be guided through obstacles. And exploiting the advantage of continuum robots, the ability to take every configuration in the workspace, obstacles that are already past will have no effect on further

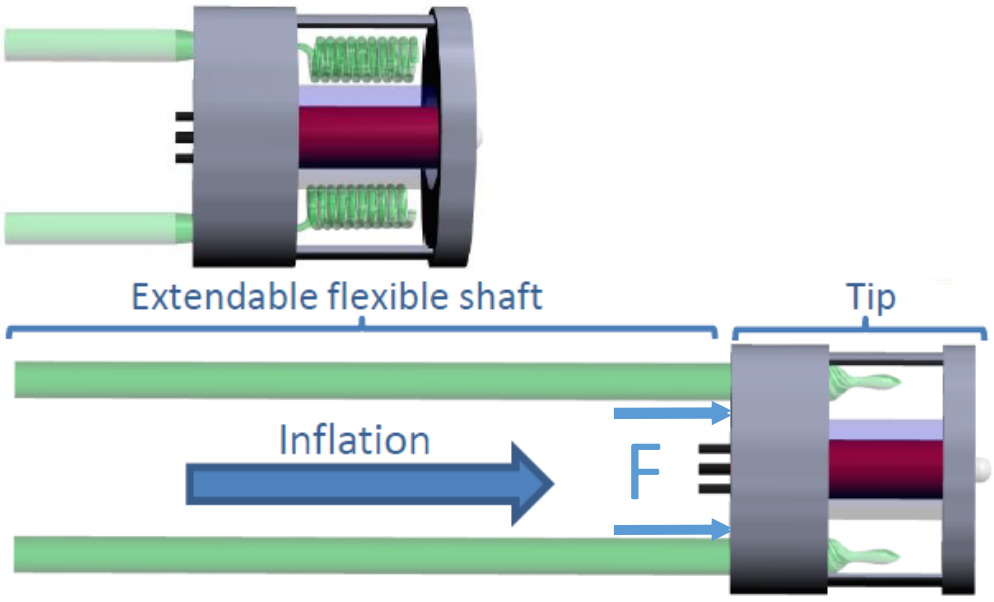

Figure 3.4. Inflation of the balloons results in elongation. The force applied on the tip pushes it forward.

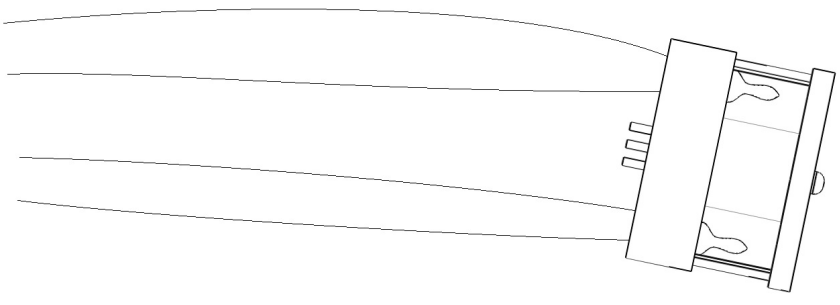

Figure 3.5. When the top balloon is inflated more than the bottom one, the tip is inclined downwards.

navigation. The robot therefore will take the shape of an appropriate curve, making it conform to the obstacle. This behaviour is depicted in Figure 3.6.

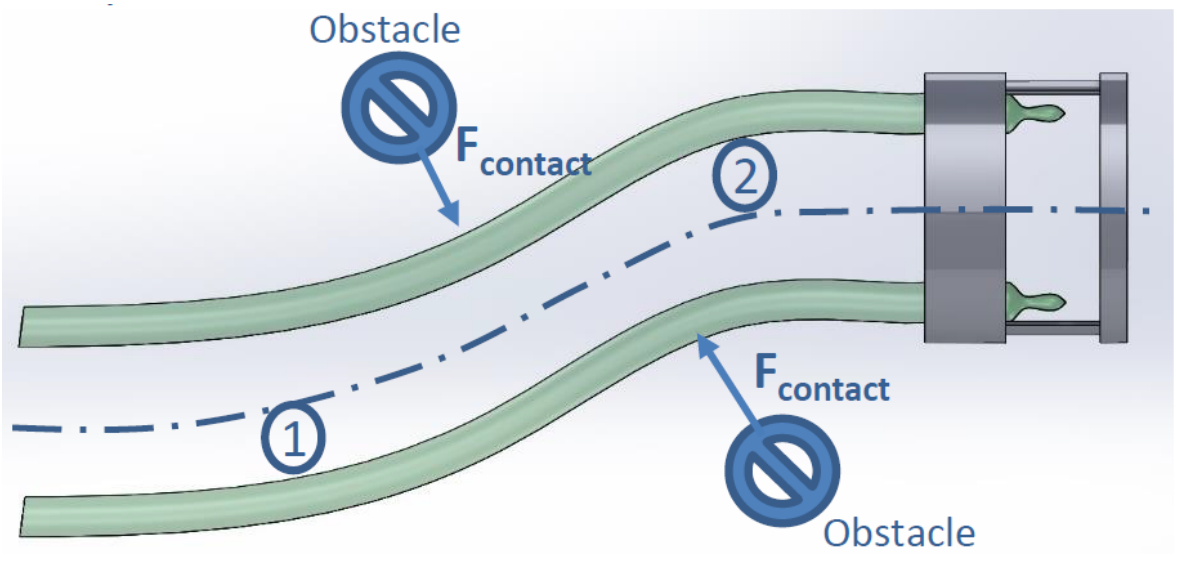

Figure 3.6. Navigation through obstacles is demonstrated. In region 1, the lower balloon is inflated more in order to have a curvature to avoid upper obstacle. In region 2, the upper balloon is inflated more to avoid lower obstacle.

4. SYSTEM OVERVIEW

4.1. Extendable Balloons

The extendable balloons used in this study are Qualatex® extendable balloons. They are made of latex and primarily used for entertainment purposes. As mentioned in Chapter 3, they have an unusual elongation mechanism. Prior to inflation, they are very soft and slack. However, during inflation only a certain section that can overcome the radial structural stiffness of the balloon under the current internal air pressure is inflated and the rest of the balloon remains slack. As more air is pumped in, the inflated section elongates and the length of the slack section decreases. Another interesting property of the balloons is that in this process, the increase in diameter is far less than the increase in length. This behaviour is depicted in Figure 3.2. When there is no slack section remaining, the balloon is still able to elongate but the radius is increasing rapidly as well. After this point, a local high strain in the membrane, especially near the inlet region may result in explosion of the balloon.

4.2. Elongation Model

In this section, mathematical model of the elongation of the robot is given. The balloon is assumed to be a single elongating cylinder as given in Figure 4.1. When air is pumped in, the length of the cylinder increases.

In this model, following assumptions are made:

- Balloon is a perfect cylinder
- Diameter is constant
- Air temperature is constant
- Ideal Gas Law [56] is applicable

The length L of the cylinder is found as a function of time t in seconds. The ideal

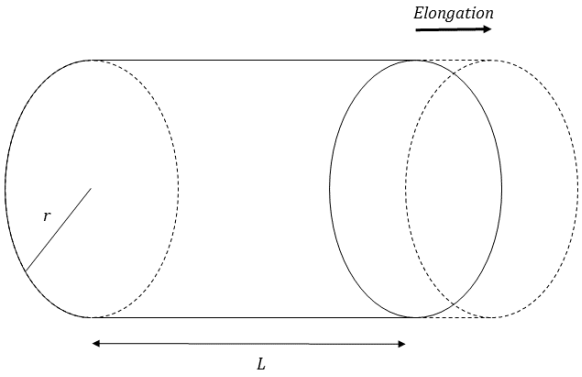

Figure 4.1. Cylindrical Model of Elongation.

gas law is given as [56]:

$$PV = nRT \tag{4.1}$$

where P is the air pressure in kPa, V is the volume of the cylinder, n is the moles of air in the cylinder, R is the universal gas constant, and T is the air temperature.

The volume of the cylinder is;

$$V = \pi r^2 L \tag{4.2}$$

where r is the radius of the cylinder.

The change of matter of air in moles in one second can be calculated as:

$$\dot{n} = \frac{PQ}{RT} \tag{4.3}$$

where Q is the air flow rate into the balloons, supplied by the air pump.

Again, applying ideal gas law, where subscripts 1 and 2 represent two consecutive states separated by a second yields combining with 4.2:

$$\frac{P_1 V_1}{n_1 RT} = \frac{P_2 V_2}{n_2 RT} \tag{4.4}$$

$$\frac{V_1}{n_1} = \frac{V_2}{n_2} \tag{4.5}$$

$$L_2 = \frac{L_1 n_2}{n_1} \tag{4.6}$$

Considering the change in moles in one second, this also means:

$$L_2 = L_1 \dot{n} \tag{4.7}$$

Then,

$$L(t) = \frac{n(t)RT}{P\pi r^2} \tag{4.8}$$

With Equation 4.8, length of a balloon in terms of seconds can be obtained.

4.3. Experimental Setup

In order to control the air in the balloons, the architecture given in Figure 4.2 is used. In this setup, there are two air pumps (Parker® BTC Diaphragm) and four two-way, normally closed solenoid valves (FG Line®) are utilized. Pumps are operated at 18 V and the valves are at 12 V DC.

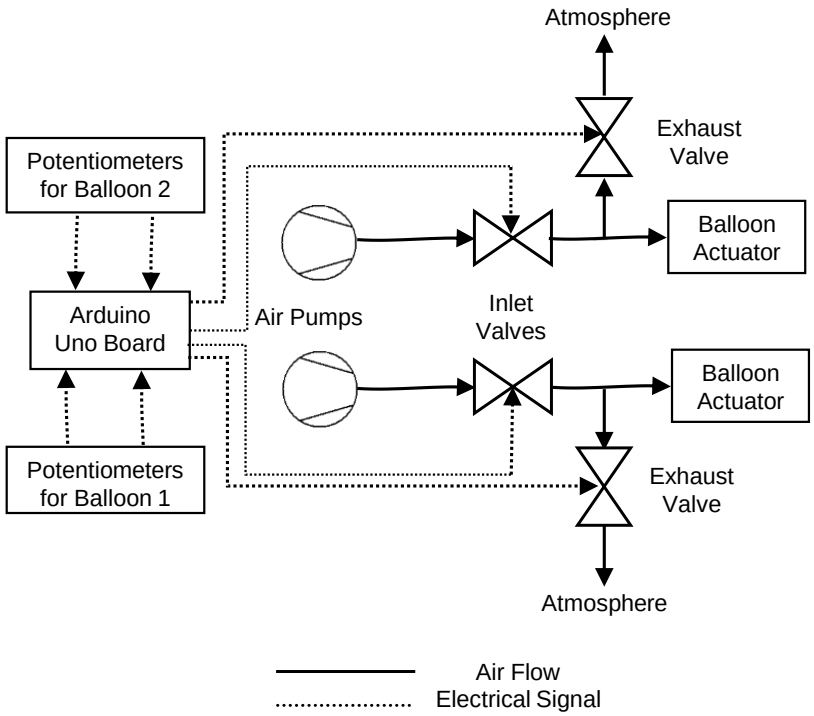

Figure 4.2. Architecture used in this study.

In order to control inflation and deflation of two balloons, two potentiometers are utilized as the user interface. Since the valves are able to work only on and off, valves are operated via Pulse Width Modulation (PWM) signals for speed control of inflation and deflation. PWM signals are generated by an Arduino® Uno Board at 1024 Hz. According to the value read from the potentiometers, each valve has three different operating regions: *on*, $on/offswitching$ and *closed*. In $on/offswitching$ mode, the on and off times are controlled by pulse widths of PWM signals. Due to their mechanical properties and effective voltages, solenoid valves are not able to track every

PWM signal, for example very low duty cycle signals. Therefore, the $on/offswitching$ region is calibrated such that the valves can always operate within a given PWM signal range.

4.4. Assembled Design

Two extendable balloons are placed in a radially constricted, axially flexible shaft. They are attached to the tip section as shown in Figure 4.3. The slack section remains outside of the tip and is retracted ever so slightly as the robot moves forward. This is because the inflated section of the balloon applies a force on the tip, pushing it forward.

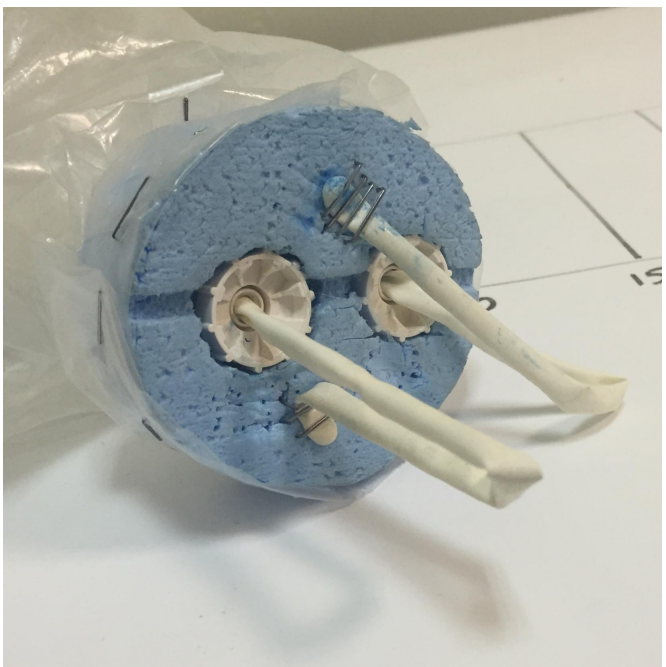

Figure 4.3. Tip of the robot made of styrofoam when the slack section remains out of the robot.

The whole experimental setup is shown in Figure 4.5. Air pumps are fed by the power supply and the solenoid valves are fed by two 12V DC power supplies. Two potentiometers are placed on a breadboard and are used to alter the duty cycle of PWM signals. PWM signals are given to the base leg of an 2N 3904 transistors. Connector leg is connected to the power adapters and the emitter leg is connected to the valves. Each potentiometer controls two solenoid valves both for inflation and deflation of each

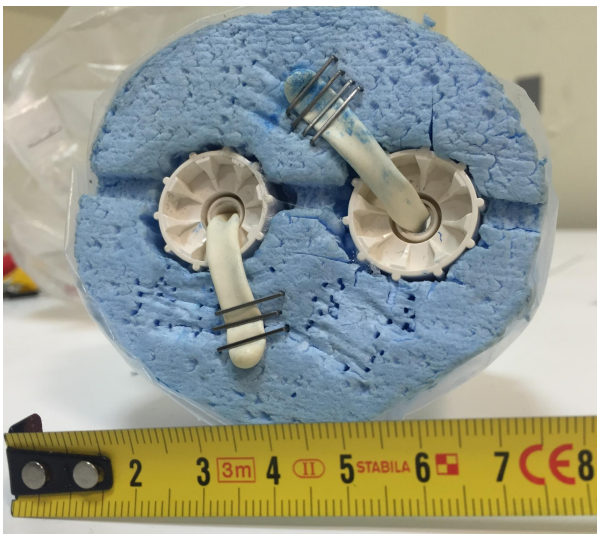

Figure 4.4. Tip of the robot made of styrofoam when the slack section is retracted.

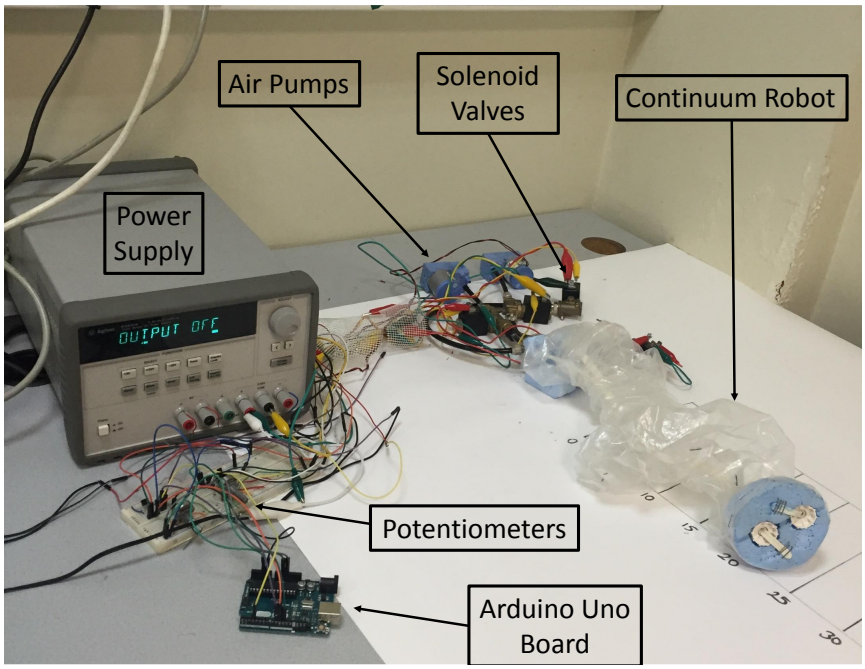

Figure 4.5. Experimental setup.

balloon. Potentiometer readings are scaled using an Arduino Uno board so that PWM signals allow the solenoid valves to operate only in a stable region where they can track input signals.

5. EXPERIMENTS AND RESULTS

5.1. Single Balloon Experiments

In this section, experiments required to find out the mechanical properties of a single balloon are carried out.

5.1.1. Elongation Measurements

In this section, the balloons are inflated by the air compressors that are working with 18V and about 330mA, corresponding to a pressure value about 18 psi. After they are fully extended, they are rapidly deflated. Displacements of the distal inflated sections were recorded. Slack sections were not considered until full expansion is reached because they are of no interest while navigating the robot. In order to get the full characteristics of the balloons, seven different balloons were used and they were inflated five times consecutively. At this point, it has to be stated that since the balloons have very high initial radial stiffness, they were preconditioned by hand pumping once so that the air compressor will have the necessary power to overcome this stiffness.

In Figure 5.1, the elongation recordings for five consecutive inflations are presented. It can be seen that there is a polynomial-like pattern. And it can be observed that after second inflation, the positions do not change much. This can be explained with the plasticity of the balloons. Their elasticity tend to converge in later inflations. During deflation, the positions tend to decrease almost at the same rate. However, at the last stages of deflation balloons may go unstable, having a slackened section between two inflated sections. If this happens, position of the farthest of the inflated sections is recorded.

The same procedure is carried out for seven balloons and their positions are recorded. Mean of five repetitions are computed for each balloon. Then, the overall mean and the standard deviations of elongation for seven balloons were calculated.

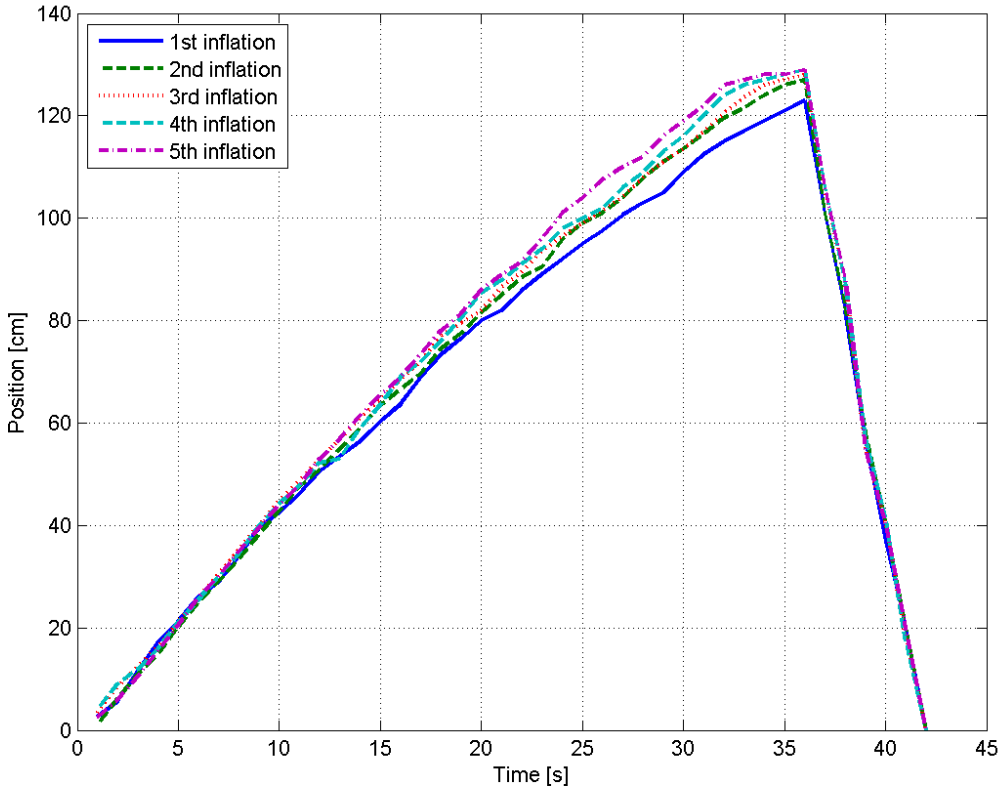

Figure 5.1. Elongation of a single balloon recorded at five consecutive inflations.

Elongation vs time graph is given in Figure 5.2. In this figure, the black line in the middle represents the mean of the positions recorded for seven balloons and the shaded region represents the standard deviation. It can clearly be seen that the balloons expand almost linearly. When they are close to full extension, when there is very little or no slack section is left, their extending speed tends to decrease and then it converges to a value of 124 $\pm$6 cm. The deviation in this value is due to individual structural properties of a balloon.

For the sake of easiness of mathematical expressions, third degree polynomials are fit into this data. These curves are given as following;

For inflation;

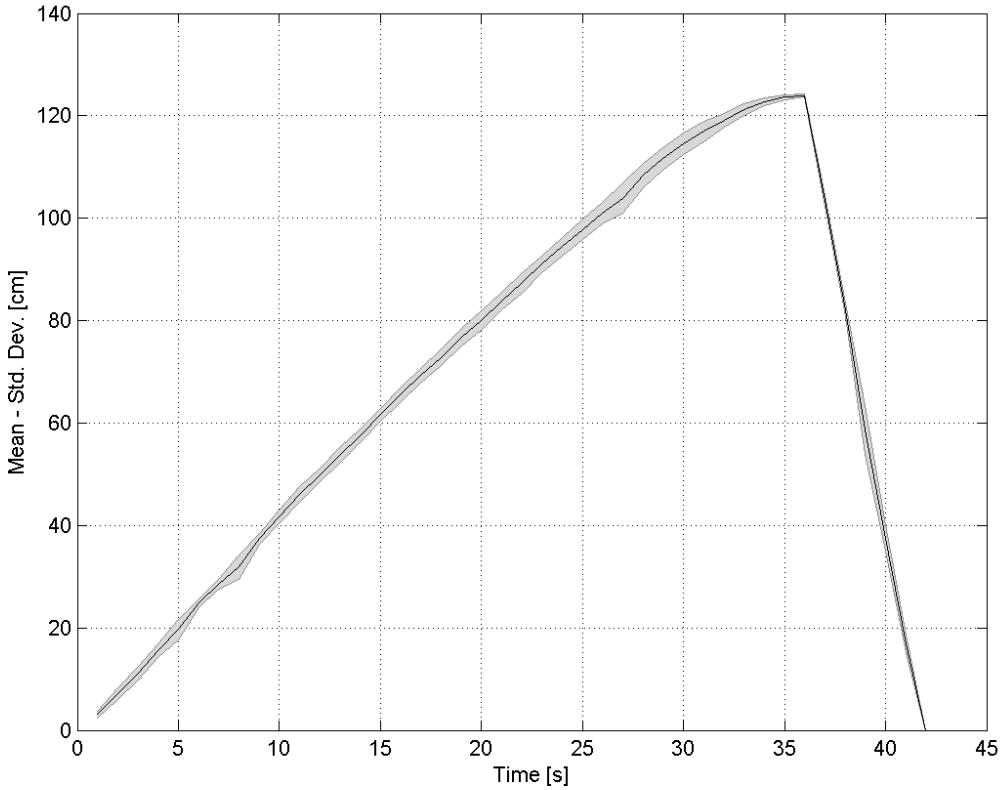

Figure 5.2. Mean and standard deviation of elongation for seven balloons.

$$P_{inf} = -0.001t^3 + 0.0221t^2 + 4.0501t - 0.7594 \tag{5.1}$$

For deflation;

$$P_{def} = -23t^2 + 857t - 10340 \tag{5.2}$$

5.1.2. Verification of Elongation Model

In this section, the model presented in Section 4.1 is verified. From the datasheet of the air compressor, the air pressure is found to be 18 psi for a current of 330mA. Details regarding the compressor are presented in Chapter 4. In SI units,

$$18psi = 124.1kPa$$

Air flow rate is modeled as linearly decreasing from 0.7 l/min to 0.65 l/min to take the slight increase in the current drawn by the pumps into account during the operation. And these values are converted to seconds.

$$Q = \frac{0.7}{60} - t\frac{0.05}{2160} \tag{5.3}$$

From Equation 4.3, with the values of R=8.314$J/Kmol$ and T=295K;

$$\dot{n} = 0.59mol/s \tag{5.4}$$

For a linear profile, this also states that:

$$n(t) = 0.59t \tag{5.5}$$

Using Equation 4.8, length of a balloon in terms of time is found as;

$$L(t) = -0.0082t^2 + 4.128t \tag{5.6}$$

In Figure 5.3, the elongation model given in Equation 5.6 is plotted.

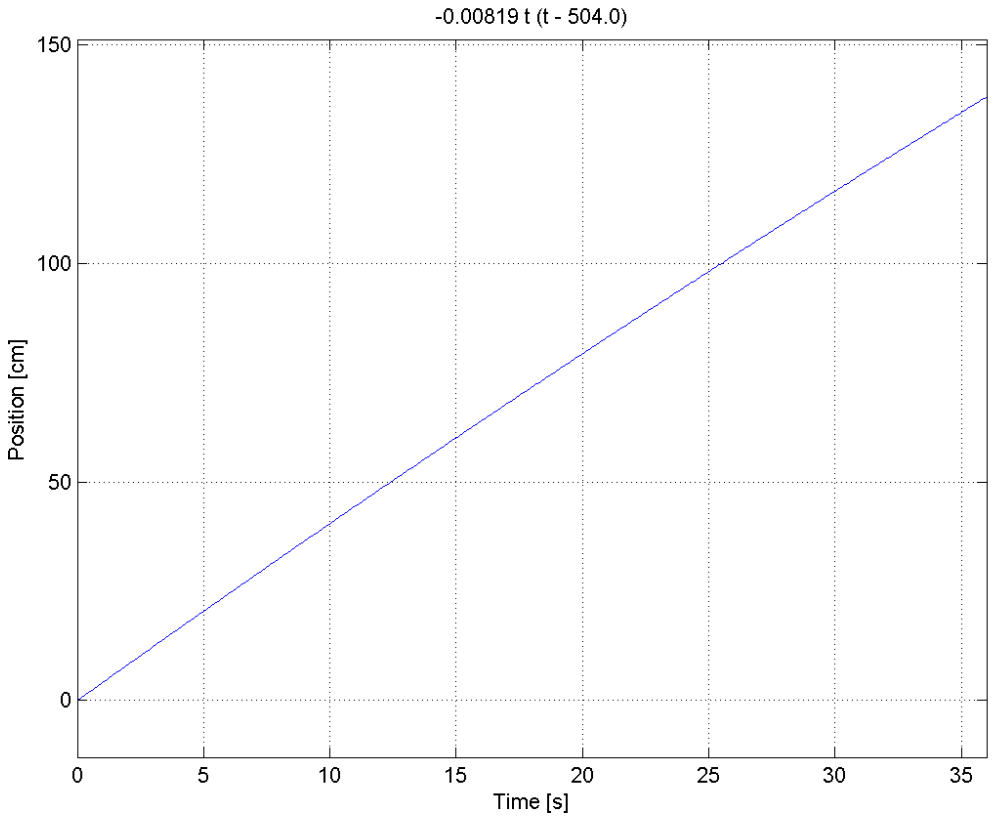

Figure 5.3. Plot of elongation model given in Equation 5.6.

In Figure5.4, Equation 5.6 is plotted together with the mean and standard deviation of elongation given in Figure 5.2 in order to show the accuracy of the model. It is seen that model is accurate even though it is quite simple. When the balloon is near full extension, the discrepancy between the model and the actual measurements increase. This is due to the fact the balloons lose their ability to freely elongate since there is little or no slack section is remaining. The balloons tend to expand in all directions.

5.1.3. Speed Results

Since speed measurements resulted in noisy data, we took the derivative of the smooth polynomial fits of the elongation data to calculate speed of inflation. Equations

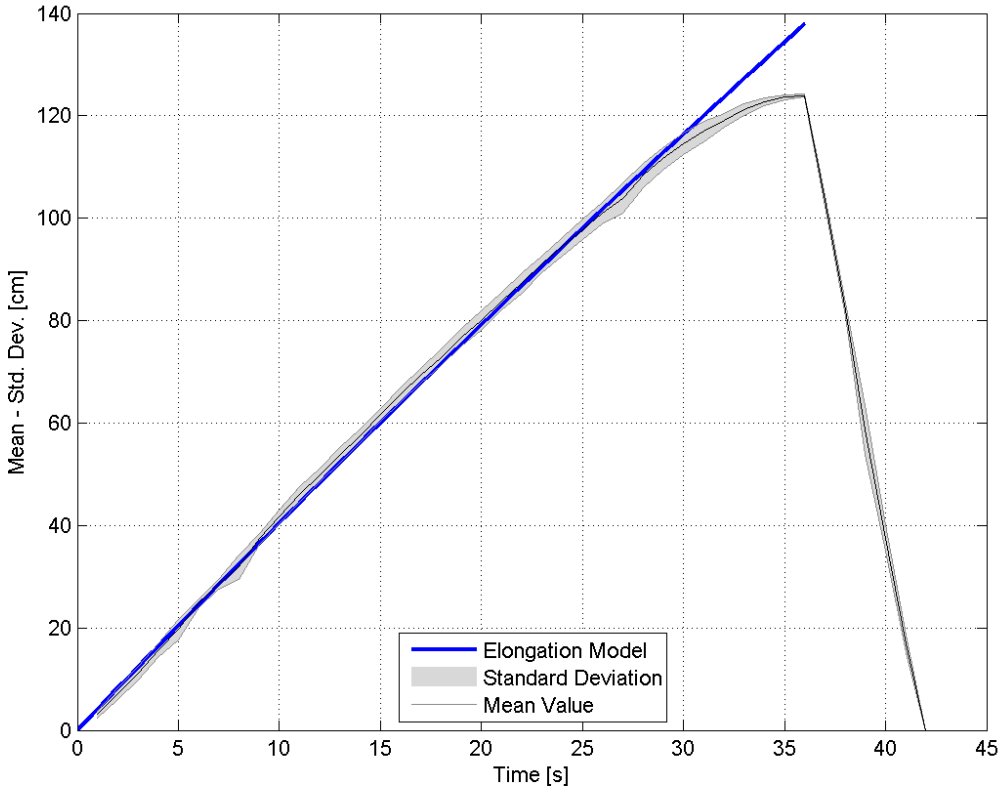

Figure 5.4. Equation 5.6 plotted on Figure 5.2.

of 2nd degree polynomials and their plots are presented in this section.

For inflation;

$$V_{inf} = -0.0031t^2 + 0.0442t + 4.0501 \tag{5.7}$$

For deflation:

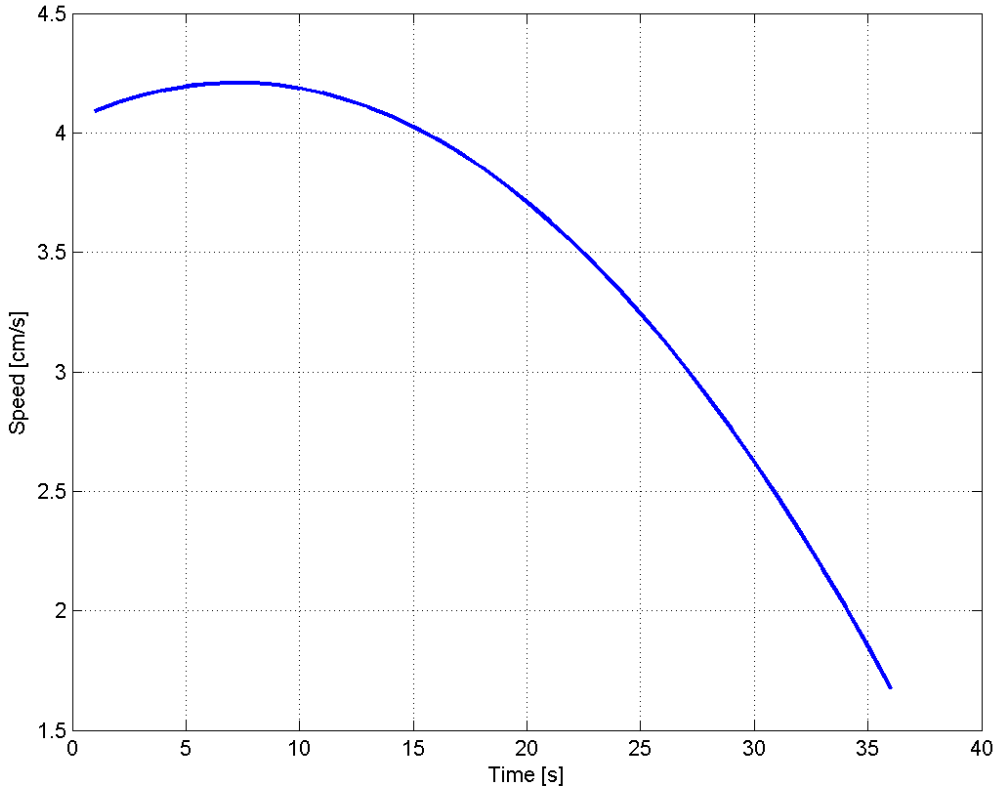

Figure 5.5. 2nd degree polynomial obtained from taking the derivative of P_{inf}.

$$V_{def} = 0.5942t^2 - 45.7262t + 857.03 \tag{5.8}$$

In Figure 5.5, the speed has a decreasing profile as expected during inflation. As the balloons get closer to their maximum position, the decrease in speed becomes much more significant. During deflation, there is a similar pattern as well. This behaviour can be clearly seen from Figure 5.6 The speed increases at first but after 13 seconds, it starts to decrease rapidly.

In order to demonstrate the effects different pulse widths on inflation, one of the balloons that was used to generate Figure 5.2 was inflated with 3 different PWM

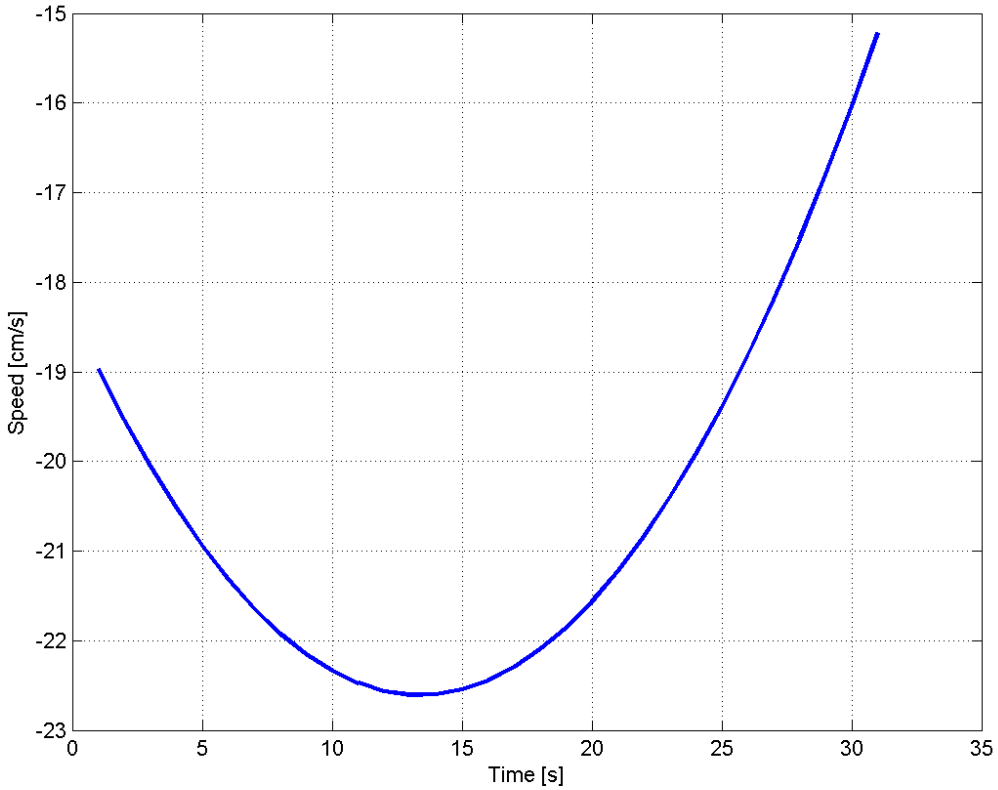

Figure 5.6. 2nd degree polynomial obtained from taking the derivative of P_{def}.

signals; 33%, 66% and 100% duty cycles of the solenoid valves. Note that these duty cycles do not correspond to the signal generated by the Arduino Uno Board since the valves cannot track the PWM inputs of very low and very high duty cycles. These percentages are taken as the pulse widths regarding to highest and lowest duty cycles that the valves can track the input. The displacements of a single balloon under different PWM signals are plotted in Figure 5.7.

In Figure 5.7, it can be seen that speed of inflation is significantly lower when lower duty cycles are used. It is also observable that maximum longitudinal strain a balloon decreases with lower duty cycles.

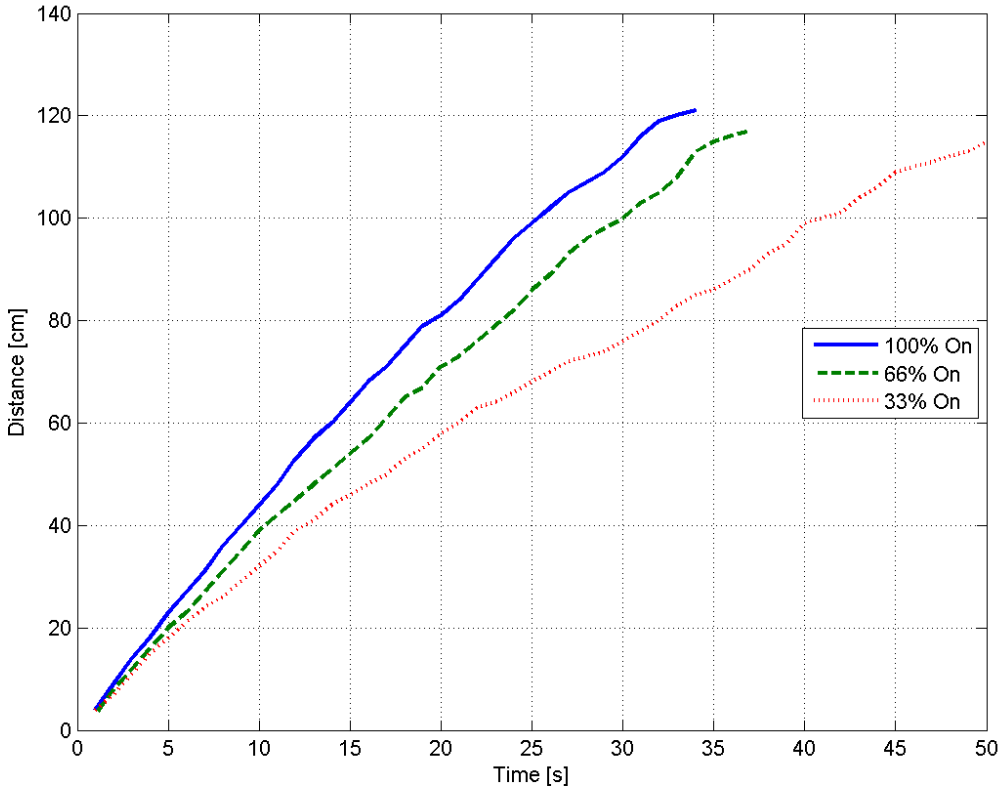

Figure 5.7. Displacements of a single balloon inflated with three duty cylces of solenoid valves.

5.1.4. Force Measurements

In this section, the force that can be applied robot was measured. In order to find the maximum force that can be applied by one balloon, the balloon was constricted in a rigid cylindrical plexiglass tube that is 1 m long. A force sensor (ATI®Nano 17) is located at the distal end of the tube. The force sensor is connected to a 3.40 Ghz 8 GB RAM computer running ATIDAQFT through National Instruments PCI-6220 DAQ card. The balloon was inflated while the valve was in fully open and the force applied at the distal end was measured for seven different balloons. It is necessary to state that the force sensor does not read any value until the balloon is 1 meter long. Therefore, the measured values are after the balloon touches the sensor. Since the balloon was constricted from radial motion, it tries only to elongate and applies force

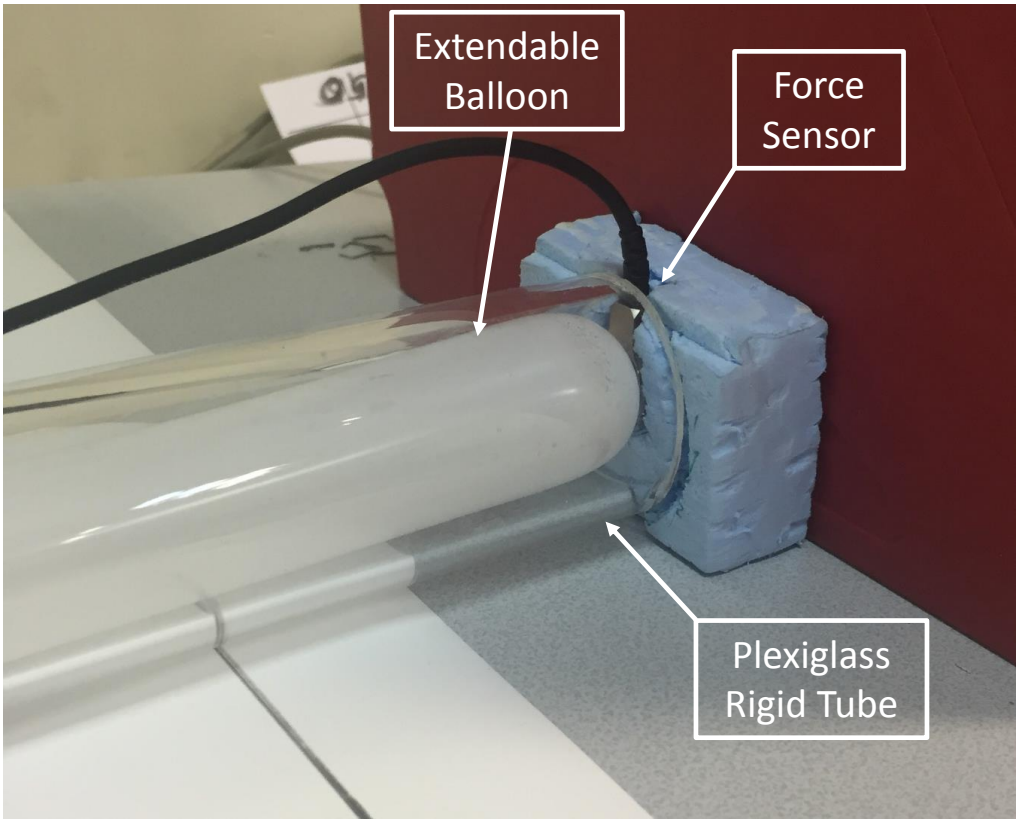

Figure 5.8. Experimental setup used to measure forc.e

on the sensor. The experimental setup is shown in Figure 5.8. The results are shown in Figure 5.9.

From Figure 5.9, it can be seen that the force values increase at a decreasing rate after the balloon touches the force sensor. After some time three of the balloons converged to a constant value of 5N and they were rapidly deflated. Similar behavior happened for balloons 4 and 6 which converged to 6.5 N. Two of the balloons (1 and 5) have exploded, which can be seen as spikes in the measured forces. The balloons ruptured from sections that are subject to high strain, especially near the inlet. This may have occured due to some defects in these regions. Even though the inside of the tube was lubricated, there was high friction between the latex balloon and the

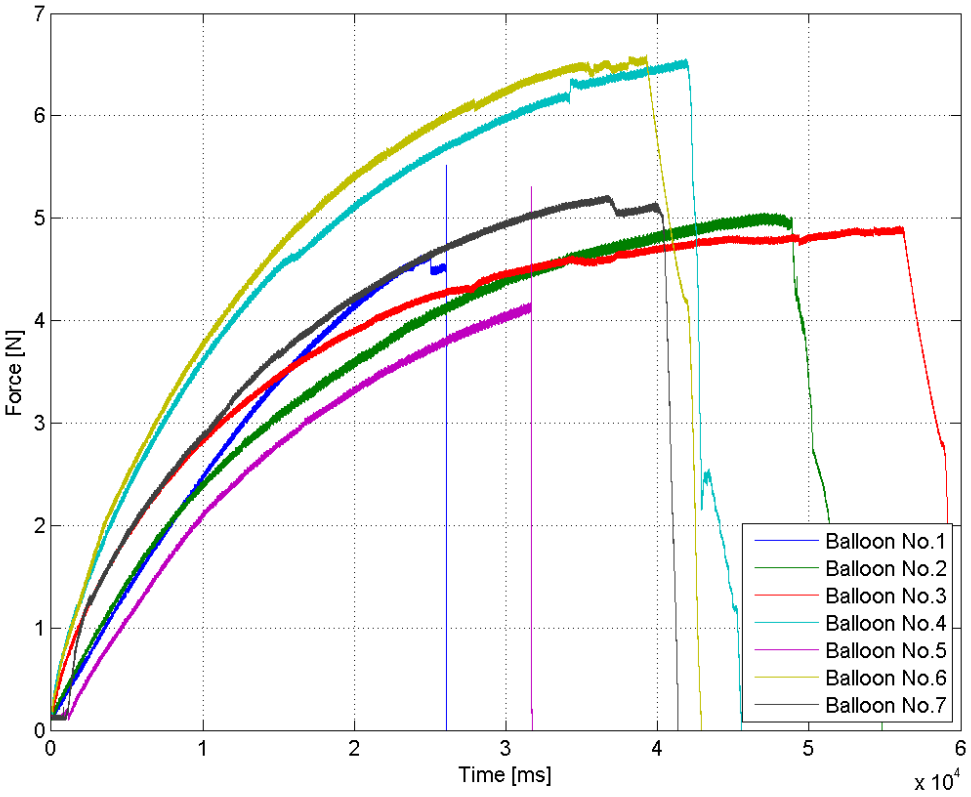

Figure 5.9. Forces measured at the distal end of a 1 m long cylindrical tube.

plexiglass tube. The sliding of the balloon over the tube surface with high friction resulted in a release in stress that caused fluctuations in the curves that can be seen in Figure 5.9.

5.2. Navigation Experiments

As explained in Section 4.4, two extendable balloons are attached to the tip of the robot from their slack sections and they are stored in a radially constricted flexible extendable shaft. In this section, navigation tests are performed and results are presented.

5.2.1. Open-Field Navigation

In this experiment, the robot was navigated in an open environment without any obstacles. As a continuum robot, it was expected to have a large-radius curvature similar to continuum robot example shown in Figure 2.3.

Firstly, the balloons were inflated together to make the robot go straight. Some side-to-side motions were encountered but they could be corrected by inflating the balloon on the same side as the curvature so that the robot could continue moving in a straight line.

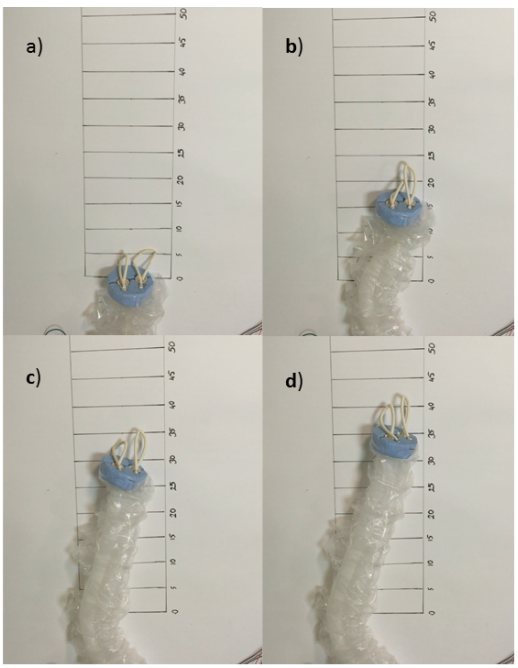

Figure 5.10. Robot elongating by inflating both balloons at the same time

Secondly, the robot was navigated to both sides by inflating a balloon more than the other. Turning to right and left are demonstrated in Figures 5.12 and 5.11, respectively.

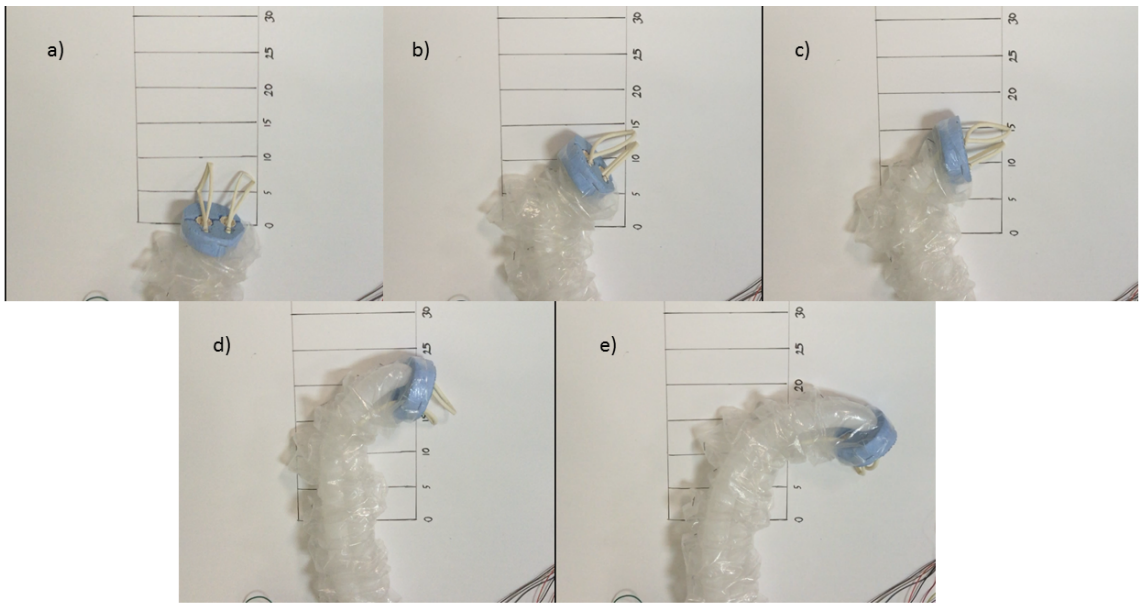

Figure 5.11. Robot turning to the right by inflating one balloon more than the other.

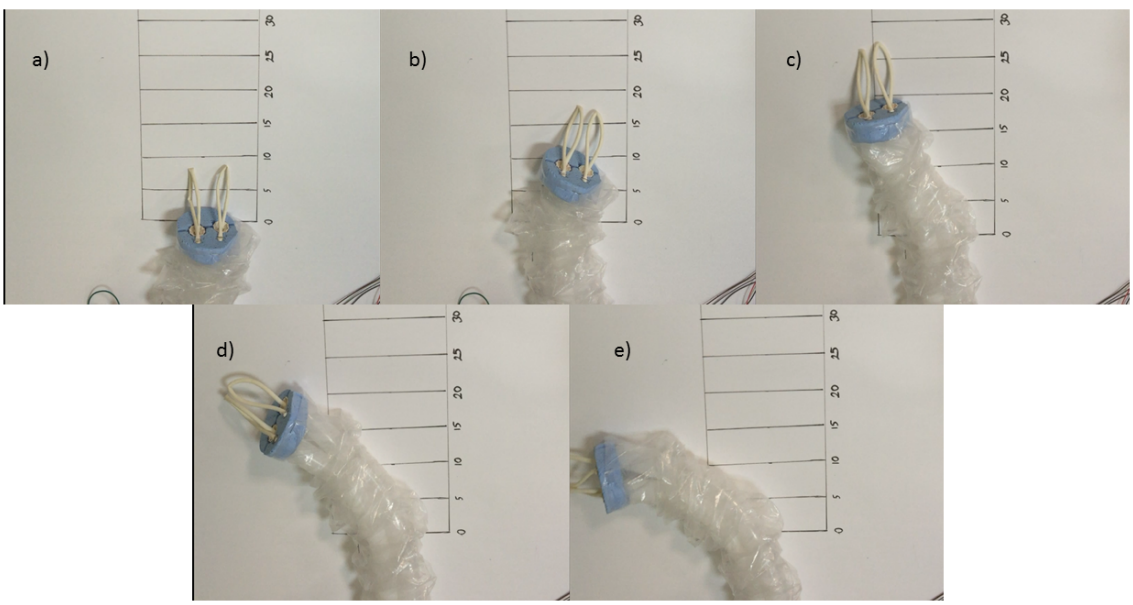

Figure 5.12. Robot turning to the left by inflating one balloon more than the other.

5.2.2. Maze Navigation

In this test, the robot was navigated through a predesigned maze-like environment to reach a goal position in the middle of the maze. The top view sketch of the maze and its dimensions are shown in Figure 5.13. The maze was manufactured from 3 mm thick plexiglass. Each wall has a height of 15 cm.

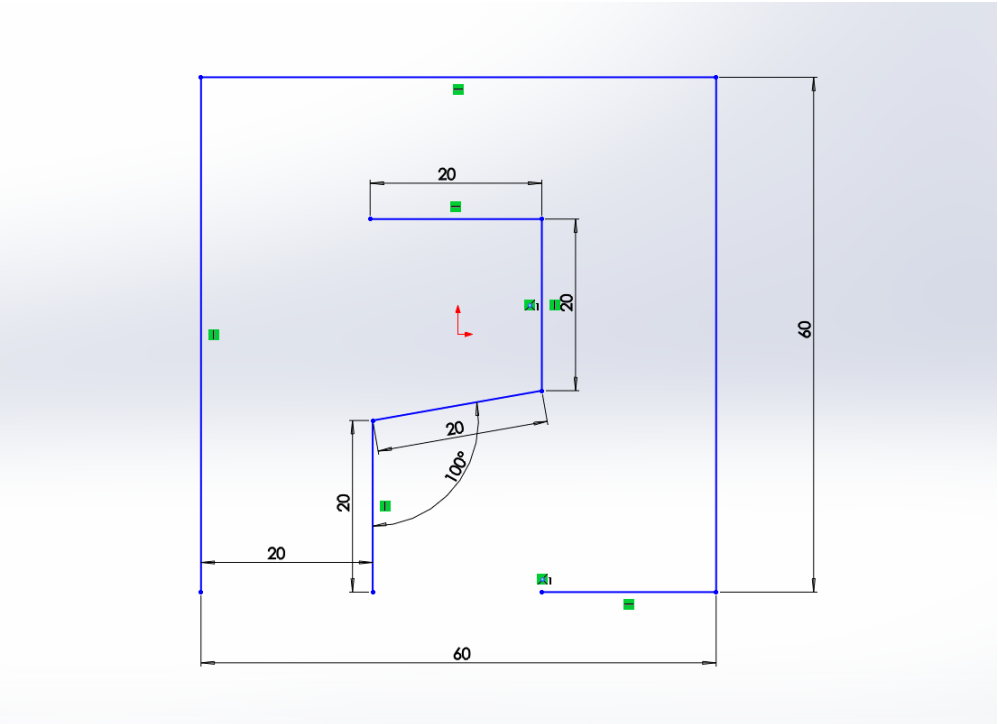

Figure 5.13. Sketch of the maze designed. (Dimensions are in cm)

The robot was placed at its initial position. It was guided through the maze by using potentiometers that control the air flow rate into each balloon. The process of reaching the goal position is demonstrated in Figure 5.14. In 5.14a, the left hand side balloon was inflated more than the one on the right so that the robot could rotate rightwards. When the configuration shown in 5.14c was reached, the balloon on the right was inflated more. However, since it is a tight corner, the balloon on the left was slightly deflated. Same operation was performed in the configuration shown in 5.14f as well.

This experiment clearly demonstrated that this robot actuated with a novel method can be successfully navigated through such an environment. However, some problems were encountered as well. In some attempts, cornering has been hard due to the crimpled structure of the flexible shaft. When the slack sections squeezed under the tip resulted in a braking force due to friction and the tip inclined towards the floor. This behaviour disrupted 2D characteristics of the robot and made it uncontrollable after that point. Finally, in some trials, when the robot was near full extension, balloon rupture was encountered. This may be explained with a defect in the balloon, in a region where high strains are seen.

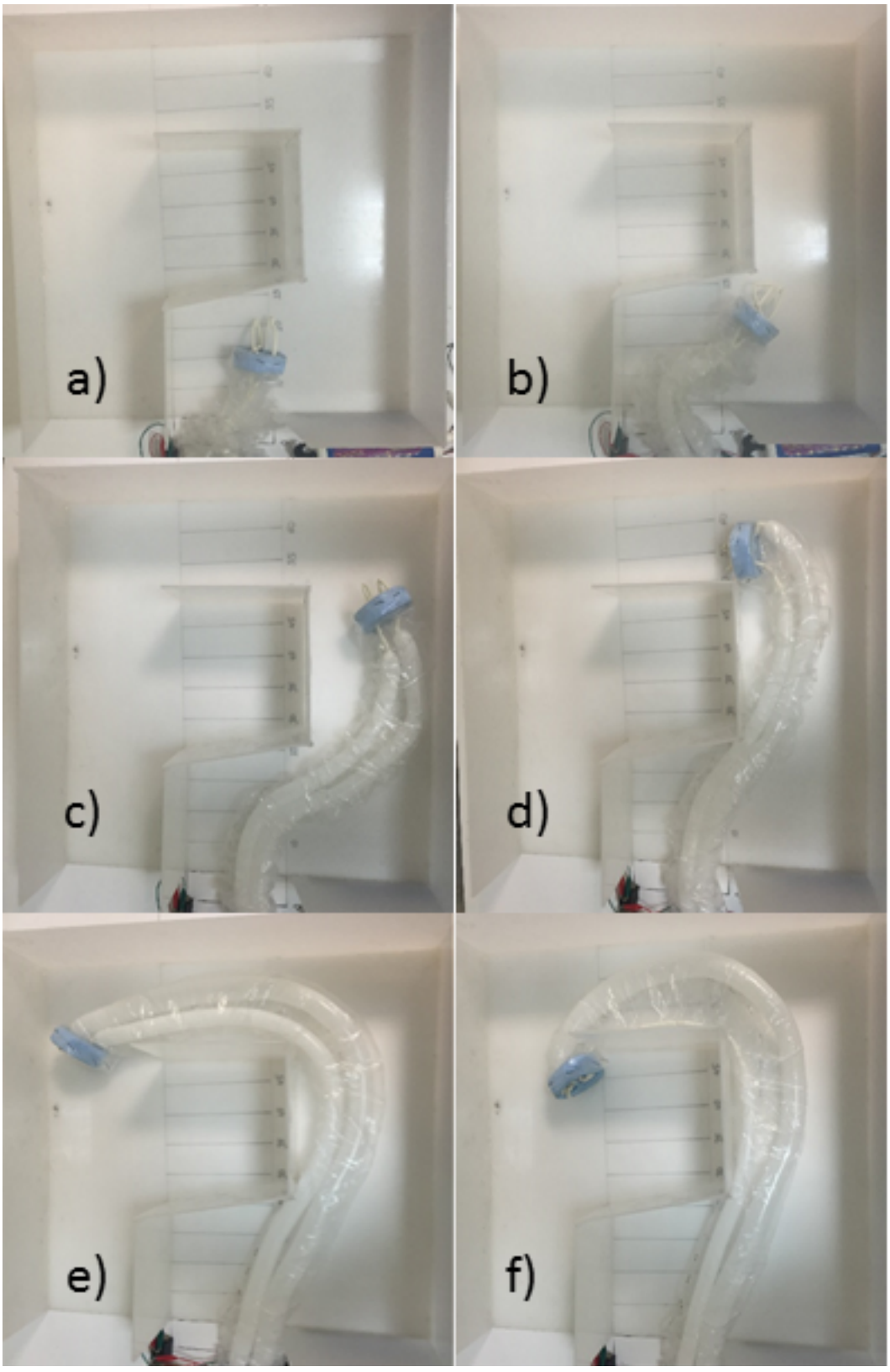

Figure 5.14. Robot navigating through a maze-like environment.

6. CONCLUSION

In this study, a novel continuum robot actuated by two extendable balloons have been designed and developed. The balloons used in the robot and the robot itself were experimentally evaluated in order to characterize extendable balloons and to test navigation abilities of the robot.

The proposed continuum robot consists of two extendable balloons restricted in a flexible shaft and a tip section. The balloons were attached to the tip from their slack sections. Air volume in balloons were controlled via two solenoid valves for each balloon, one for inlet and the other one for exhaust. Air flow rate into each balloon were controlled by sending PWM signals to the valves. Air was supplied by an air compressor.

The balloons used in the study were analyzed. Their displacement and force characteristics were measured. Then, the robot has been set up and was tested in an open field to perform two basic motions: elongation and bending. Finally, it was tested in a maze-like environment to complete several turns in order to reach a goal position.

6.1. Contributions and Originality

In this study, a continuum robot has been developed with a new kind of pneumatic actuation. The robot was controlled by changing the air volume in two extendable balloons. The main advantage of the novel design is that the actuation system allowed the robot to have much more longitudinal strain than the examples in the literature. Since the backbone of the robot is guided by the obstacles in the workspace, it can reach a goal position very fast, especially in substantially long and narrow environments.

A patent regarding the conceptual design presented in Section 3 has been filed to Turkish Patent Institute with no. 2015/02185 under the name "A Medical Device for Colonoscopy". Its status is currently pending.

6.2. Outlook and Future Work

This novel robot presents certain advantages mentions over robots in the literature. With further investigation, it can be developed in many ways. In the future, an advanced and homogeneous polymer can be employed instead of off-the-shelf extendable balloons. This may allow a more controllable and robust motion. Moreover, if the polymer can be tailored in different sizes, the robot can be employed for many different purposes, such as exploratory or medical purposes. A more advanced material can be utilized as the flexible shaft such that the balloons can be constricted more tightly to provide better control and less irregular contact with the obstacles. Finally, some kind of stiffening mechanism like jamming may introduce load bearing capability.

With the more advanced design and careful regulation of air volumes in the balloons, it should become quite easy to navigate the robot, especially through delicate cavities. Then, type of robots can be utilized in various fields by having necessary tools attached on the tip. Especially in the exploratory, diagnostic or medical applications where the objective is to reach a goal position and carry out tasks there without applying much force to the walls of the cavities, this novel design can be used as a videoscope or an endoscope providing a great advancement in the existing technology.

APPENDIX A: DATASHEETS

Parker

Part No.: **H022C-11**
Model No.: **B.1F32E1.A12VDC**
Description: **BTC Diaphragm Pump, Brushless Motor**

Mooresville, North Carolina 28117
T: 704-662-3500 F: 704-662-8744
www.hargravesfluidics.com

Dimensional Layout:

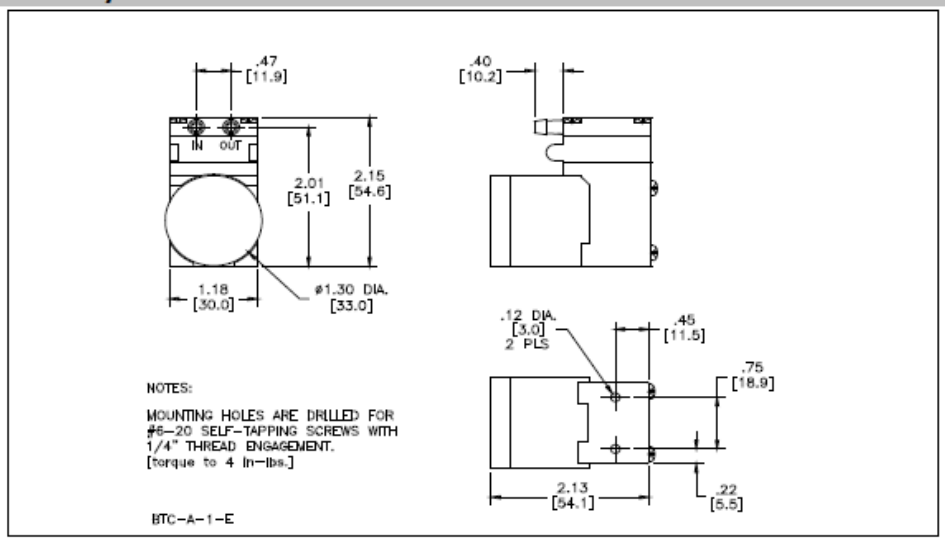

Specifications:

1. Wetted Materials:	Pump Head:	Vectra [LCP]
	Retainer Washer:	303 Stainless [800]
	Retainer Screw:	316 Stainless
	Valves:	EPDM [Q55]
	Diaphragm:	AEPDM [F80]
	Gasket:	EPDM [65]

2. Performance:	Continuous	Maximum
- Vacuum: in Hg [AIR]	18.0	18.0
- Pressure: PSIG [AIR]	24.0	24.0

3. Electrical:	Motor:	Brushless Dual Bearing
	Operating Voltage:	12.0 VDC
	In-rush Current:	5 x Operating Current for up to 50 ms
	Recommended Fusing:	Slow Blow @ 2 x Operating Current

4. Other:	Temperature Range:	5 - 50° C
	Free Flow RPM:	3500
	Eccentric:	A465

5. Operating Limitations: N/A

6. Recommended Filtration: 40 Micron media w/ a minimum surface area of .39"Sq (252mmSq)

Figure A.1. Data sheet of the air pump, part 1.

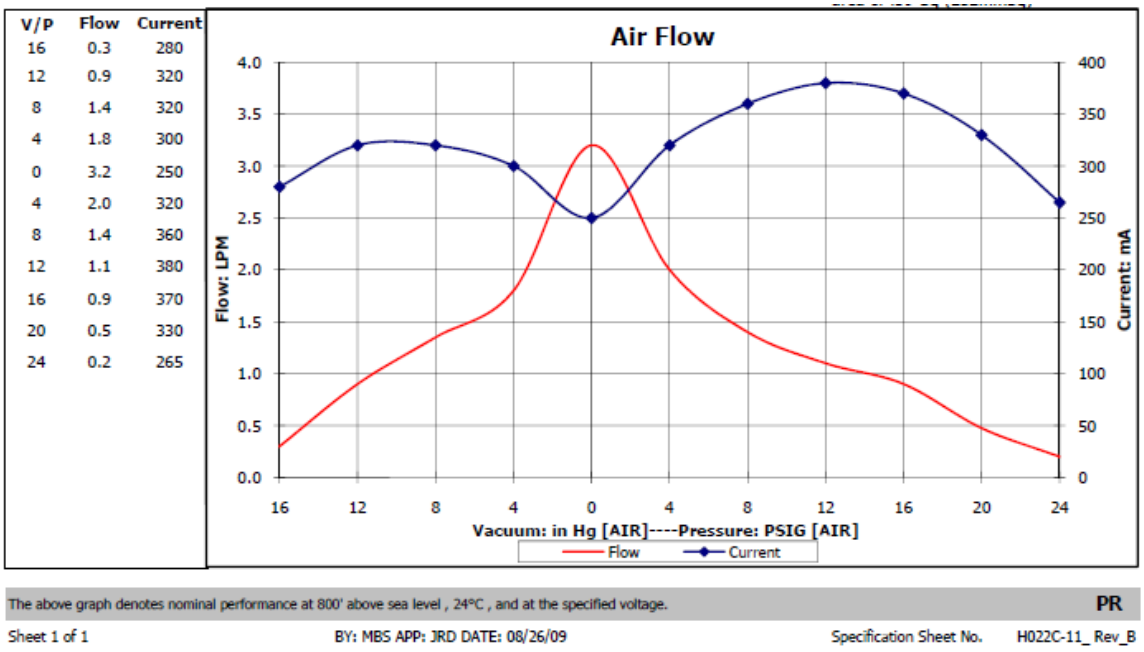

Figure A.2. Data sheet of the air pump, part 2.

THREE WAY NORMALLY CLOSED DIRECT ACTING SOLENOID VALVE

C01

GENERAL DESCRIPTION / APPLICATIONS

Three way direct acting solenoid valve with spring return, normally close.

Suitable for gaseous and liquid media compatible with the used material (body/seals), vacuum.

Forged brass body.
Brass guide tube.
Stainless steel internal parts.
Stainless steel springs.

Solenoid can be rotated 360°.

Valve will operate in any position.

DIMENSIONS mm

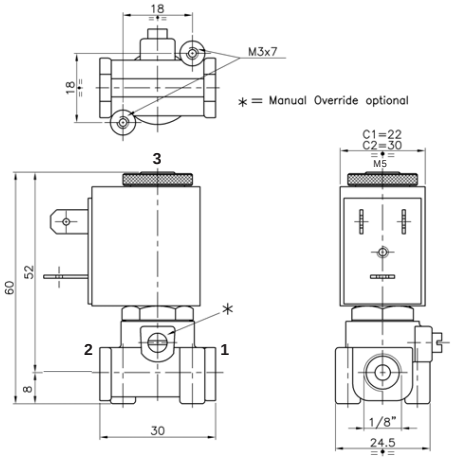

ELETTRICAL INFORMATIONS

Continuous duty glass-reinforced nylon mouldedcoil with electrical connection suitable for DIN-43650 plug (2 poles+ground) or faston wire terminal . Two cables available on request.

Coil type:	C1
Insulation class:	F (155°C), H (180°C) on request.
Winding wire class:	H (180°C)
Protection class:	Waterproof IP-65 (norme EN60529) when properly plug connetted when DIN-43650 plug.
Duty:	Continuous (S.I.) 100% ED
Power consumption:	Alternate Current 8VA (inrush 12VA) Direct Current 5,5W
Voltage tollerance:	a.c. +10% ÷ -15%, d.c. +10% ÷ -5%
Elettrical Insulation:	>500 MOhm
Dielectrical Strenght:	>2000 V/1'
Standard voltage:	d.c. 12, 24 Volt a.c. 24, 110, 230 Volt (50/60 Hz) other voltages available on request.

OPERATION

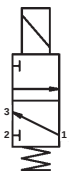

Normally closed

In :	2
Out :	1
Vent :	3
Coil de-energised :	Input 2 closed From 1 to vent 3
Coil energised :	From 2 to 1 Vent 3 closed

SPECIFICATIONS AND AVAILABLE OPTIONS

MODEL (a b c d e f)	ORIFICE mm	BODY RATING MAX.	PRESSURES IN BAR — MIN. / MAX. DIFFERENZIAL PRESSURES MIN.	MAX. AC~	MAX. DC=	Flow factor kv (liters/min.')	Weight Kg
C 01 B 12	1,2 (1,2)	15	0	15	15	0,65	0,14
C 01 B 15	1,5 (1,5)	10	0	10	10	1	0,14
C 01 B 20	2,0 (1,9)	6	0	6	6	1,5	0,14

a Construction	b Valve type	c Port size G	d Seals material	e Body material	f Optional feature
A AC C DC	C 3 way	B 2 and 1 : 1/8" GAS 3 : M5	B NBR V VITON E EPDM	T Brass N Nichel-plated brass	M Manual override SG Clean for oxigene I Stainless steel guide tube

FG line srl - Via dell'Industria, 32/36 - 24126 Bergamo (BG) - Italy Tel. +39 035 322441 - Fax +39 035 322439 - Internet: www.fgline.it e-mail: fgline@fgline.it

Figure A.3. Data sheet of the solenoid valve.

REFERENCES

1. Grossard, M., N. Chaillet and S. Regnier, "Flexible Robotics", pp. 349–379, London, UK, nov 2013.

2. Sanan, S., *Soft Inflatable Robots for Safe Physical Human Interaction*, Phd thesis, Carnegie Mellon University, 2013.

3. Loeve, A., P. Breedveld and J. Dankelman, "Scopes too flexible ... and too stiff", *IEEE Pulse*, Vol. 1, No. 6, pp. 2154–2287, 2010.

4. Aron, M. and M. M. Desai, "Flexible robotics.", *The Urologic clinics of North America*, Vol. 36, No. 2, pp. 157–62, viii, 2009.

5. Fisher, D. a., J. T. Maple, T. Ben-Menachem, B. D. Cash, G. A. Decker, D. S. Early, J. a. Evans, R. D. Fanelli, N. Fukami, J. H. Hwang, R. Jain, T. L. Jue, K. M. Khan, P. M. Malpas, R. N. Sharaf, A. K. Shergill and J. a. Dominitz, "Complications of colonoscopy", *Gastrointestinal Endoscopy*, Vol. 74, No. 4, pp. 745–752, oct 2011.

6. Cianchetti, M., T. Ranzani, G. Gerboni, T. Nanayakkara, K. Althoefer, P. Dasgupta and A. Menciassi, "Soft Robotics Technologies to Address Shortcomings in Today's Minimally Invasive Surgery: The STIFF-FLOP Approach", *Soft Robotics*, Vol. 1, No. 2, pp. 122–131, 2014.

7. Trivedi, D., C. D. Rahn, W. M. Kier and I. D. Walker, "Soft robotics: Biological inspiration, state of the art, and future research", *Applied Bionics and Biomechanics*, Vol. 5, No. 3, pp. 99–117, 2008.

8. Gera, D. L., *Ancient Greek ideas on speech, language, and civilization*, Oxford University Press, New York, USA, 1st edn., 2003.

9. Hornby, A. S., A. P. Cowie and A C Gimson, "Oxford Advanced Learning Dictionary of Current English", , 1987.

10. Weiner, T., "A New Model Army Soldier Rolls Closer to the Battlefield", *New York Times*, p. 2, 2005.

11. Corke, P. and J. Roberts, "Mining robotics", *Springer Handbook of Robotics*, pp. 1127–1150, 2008.

12. Groover, M., "Automation, Production Systems, and Computer-Integrated Manufacturing", *Automation, Production Systems, and Computer-integrated Manufacturing*, p. 290, 2008.

13. Rosen, J., B. Hannaford and R. M. Satava, *Surgical robotics: Systems applications and visions*, 2011.

14. Mukai, T., M. Onishi, T. Odashima, S. Hirano and Z. L. Z. Luo, "Development of the Tactile Sensor System of a Human-Interactive Robot "RI-MAN"", *IEEE Transactions on Robotics*, Vol. 24, No. 2, pp. 505–512, 2008.

15. Pratt, G. and M. Williamson, *Series elastic actuators*, Master thesis, Massachusetts Institute of Technology, 1995.

16. Haddadin, S., A. Albu-Schaffer and G. Hirzinger, "Requirements for Safe Robots: Measurements, Analysis and New Insights", *The International Journal of Robotics Research*, Vol. 28, No. 11-12, pp. 1507–1527, 2009.

17. Cannon, R. H. and E. Schmitz, "Initial Experiments on the End-Point Control of a Flexible One-Link Robot", *The International Journal of Robotics Research*, Vol. 3, No. 3, pp. 62–75, 1984.

18. Feliu, V., E. Pereira and I. M. Díaz, "Passivity-based control of single-link flexible manipulators using a linear strain feedback", *Mechanism and Machine Theory*,

Vol. 71, pp. 191–208, 2014.

19. Shawky, A., D. Zydek, Y. Z. Elhalwagy and A. Ordys, "Modeling and nonlinear control of a flexible-link manipulator", *Applied Mathematical Modelling*, Vol. 37, No. 23, pp. 9591–9602, 2013.

20. Albu-Schaffer, A., O. Eiberger, M. Grebenstein, S. Haddadin, C. Ott, T. Wimbock, S. Wolf and G. Hirzinger, "Soft robotics", *IEEE Robotics & Automation Magazine*, Vol. 15, No. 3, pp. 20–30, 2008.

21. Walker, I. D., "Some Issues in Creating ' Invertebrate ' Robots", *Int. Symp. Adaptive Motion of Animals and Machines*, , No. 2, p. 6 pp., 2000.

22. Wei, Y., Y. Chen, Y. Yang and Y. Li, "A soft robotic spine with tunable stiffness based on integrated ball joint and particle jamming", *Mechatronics*, pp. 1–9, 2015.

23. Cheng, N. G., M. B. Lobovsky, S. J. Keating, A. M. Setapen, K. I. Gero, A. E. Hosoi and K. D. Iagnemma, "Design and analysis of a robust, low-cost, highly articulated manipulator enabled by jamming of granular media", *Proceedings - IEEE International Conference on Robotics and Automation*, pp. 4328–4333, 2012.

24. Ranzani, T., M. Cianchetti, G. Gerboni, I. D. Falco, G. Petroni and A. Menciassi, "A modular soft manipulator with variable stiffness", *3rd Joint Workshop on New Technologies for Computer/Robot Assisted Surgery*, September, pp. 11–14, Verona, Italy, 2013.

25. Sadeghi, a., L. Beccai and B. Mazzolai, "Innovative soft robots based on electro-rheological fluids", *IEEE International Conference on Intelligent Robots and Systems*, pp. 4237–4242, 2012.

26. Ahmed, R. M., I. G. Kalaykov and A. V. Ananiev, "Modeling of magneto rheological fluid actuator enabling safe human-robot interaction", *IEEE International Conference on Emerging Technologies and Factory Automation, ETFA*, pp. 974–

979, 2008.

27. Wang, B. L. and F. Iida, "Deformation in Soft-Matter Robotics", *IEEE Robotics & Automation Magazine*, , No. September, pp. 125–139, 2015.

28. Walker, I. D., "Continuous Backbone "Continuum" Robot Manipulators", *ISRN Robotics*, Vol. 2013, pp. 1–19, 2013.

29. Chirikjian, G., "Hyper Redundant Manipulator Dynamics", *Advanced Robotics*, Vol. 9, No. 3, pp. 217–243, 1995.

30. Kier Kathleen K., W. M. and Smith, "Tongues, tentacles and trunks: the biomechanics of movement in muscular-hydrostats. Zoological Journal of the Linnean Society, London, 83: 307-324.", *Zoological Journal of the Linnean Society*, Vol. 83, pp. 307–324, 1985.

31. Katz, D., Y. Pyuro and O. Brock, "Learning to Manipulate Articulated Objects in Unstructured Environments Using a Grounded Relational Representation", *Robotics: science and systems IV*, p. 254, 2009.

32. Liljebäck, P., Ø. Stavdahl, K. Y. Pettersen and J. T. Gravdahl, "Two new design concepts for snake robot locomotion in unstructured environments", *Paladyn, Journal of Behavioral Robotics*, Vol. 1, No. 3, pp. 154–159, 2010.

33. Robinson, G. and J. Davies, "Continuum robots - a state of the art", *Proceedings 1999 IEEE International Conference on Robotics and Automation (Cat. No.99CH36288C)*, Vol. 4, No. May, pp. 2849–2854, 1999.

34. Van Varseveld, R. B. and G. M. Bone, "Accurate position control of a pneumatic actuator using on/off solenoid valves", *IEEE/ASME Transactions on Mechatronics*, Vol. 2, No. 3, pp. 195–204, 1997.

35. Caldwell, D., G. Medrano-Cerda and M. Goodwin, "Braided pneumatic actuator

control of a multi-jointed manipulator", *Proceedings of IEEE Systems Man and Cybernetics Conference - SMC*, pp. 423–428, 1993.

36. Simaan, N., Kai Xu, Wei Wei, A. Kapoor, P. Kazanzides, R. Taylor and P. Flint, "Design and Integration of a Telerobotic System for Minimally Invasive Surgery of the Throat", *The International Journal of Robotics Research*, Vol. 28, No. 9, pp. 1134–1153, 2009.

37. Richer, E. and Y. Hurmuzlu, "A High Performance Pneumatic Force Actuator System: Part II—Nonlinear Controller Design", *Journal of Dynamic Systems, Measurement, and Control*, Vol. 122, No. 3, p. 426, 2000.

38. Chou, C.-P. and B. Hannaford, "Measurement and Modeling og McKibben Pneumatic Artificial Muscles", *IEEE Transactions on Robotics and Automation*, Vol. 12, No. 1, pp. 90–102, 1996.

39. Daerden, F. and D. Lefeber, "Pneumatic artificial muscles: actuators for robotics and automation", *European Journal of Mechanical and Environmental Engineering*, Vol. 47, No. 1, pp. 11–21, 2002.

40. Salomonski, N., M. Shoham and G. Grossman, "Light Robot Arm Based on Inflatable Structure", *CIRP Annals - Manufacturing Technology*, Vol. 44, No. 1, pp. 87–90, 1995.

41. Voisembert, S., a. Riwan, N. Mechbal and a. Barraco, "A novel inflatable robot with constant and continuous volume", *Proceedings - IEEE International Conference on Robotics and Automation*, pp. 5843–5848, 2011.

42. Qi, R., T. L. Lam and Y. Xu, "Mechanical design and implementation of a soft inflatable robot arm for safe human-robot interaction", *2014 IEEE International Conference on Robotics and Automation (ICRA)*, , No. Iros, pp. 3490–3495, 2014.

43. Qi, R., T. L. Lam and Y. Xu, "Mechanical design and implementation of a soft

inflatable robot arm for safe human-robot interaction", *2014 IEEE International Conference on Robotics and Automation (ICRA)*, pp. 3490–3495, 2014.

44. Chirikjian, G. S., *Theory and applications of hyper-redundant robotic manipulators*, Phd thesis, California Institute of Technology, 1992.

45. Chirikjian, G. and J. Burdick, "A hyper-redundant manipulator", *IEEE Robotics & Automation Magazine*, Vol. 1, No. 4, pp. 22–29, 1994.

46. Mehling, J., M. Diftler, M. Chu and M. Valvo, "A Minimally Invasive Tendril Robot for In-Space Inspection", *The First IEEE/RAS-EMBS International Conference on Biomedical Robotics and Biomechatronics, 2006. BioRob 2006.*, Vol. 2006, pp. 690–695, 2006.

47. Swaney, P. J., A. W. Mahoney, A. A. Remirez, E. Lamers, B. I. Hartley, R. H. Feins, R. Alterovitz and R. J. {Webster III}, "Tendons, concentric tubes, and a bevel tip: three steerable robots in one transoral lung access system", *IEEE Int. Conf. Robotics and Automation (ICRA)*, pp. 5378–5383, 2015.

48. Pritts, M. and C. Rahn, "Design of an artificial muscle continuum robot", *IEEE International Conference on Robotics and Automation, 2004. Proceedings. ICRA '04. 2004*, Vol. 5, No. April, pp. 4742–4746, 2004.

49. Falco, I. D., A. Menciassi and M. Cianchetti, "Stiff-flop surgical manipulator: design and preliminary motion evalutaion", *4th Joint Workshop on New Technologies for Computer/Robot Assisted Surgery*, pp. 131–134, Genoa, Italy, 2014.

50. Czarnowski, J., M. Macia, J. Główka, M. Cianchetti and A. Menciassi, "New STIFF-FLOP module construction idea for improved actuation and sensing", pp. 2901–2906, 2015.

51. Bishop-Moser, J., G. Krishnan, C. Kim and S. Kota, "Design of soft robotic actuators using fluid-filled fiber-reinforced elastomeric enclosures in parallel combi-

nations", *IEEE International Conference on Intelligent Robots and Systems*, pp. 4264–4269, 2012.

52. Maghooa, F., A. Stilli, Y. Noh, K. Althoefer and H. A. Wurdemann, "Tendon and pressure actuation for a bio-inspired manipulator based on an antagonistic principle", *IEEE International Conference on Robotics and Automation*, pp. 2556–2561, 2015.

53. Hazar, S., *Theoretical and Numerical Analysis of Fracture of Shape Memory Alloys*, Ph.D. Thesis, Boğaziçi University, 2015.

54. Villanueva, A., C. Smith and S. Priya, "A biomimetic robotic jellyfish (Robojelly) actuated by shape memory alloy composite actuators.", *Bioinspiration & biomimetics*, Vol. 6, No. 3, p. 36004, 2011.

55. Sujan, V., "Lightweight hyper-redundant binary elements for planetary exploration robots", *IEEE/ASME International Conference on Advanced Intelligent Mechatronics Proceedings*, July, pp. 1273–1278, Como, Italy, 2001.

56. Incropera, F. P. and D. P. D. Witt, *Fundamentals of heat and mass transfer*, 1990.